

Morphodynamic model of the Meuse River

Linne - Roermond v0.5, Roermond - Belfeld v0.5, Belfeld - Sambeek v0.5,
Grave - Lith v0.5, Lith - Keizersveer v0.5



Morphodynamic model of the Meuse River

Linne - Roermond v0.5, Roermond - Belfeld v0.5, Belfeld - Sambeek v0.5,
Grave - Lith v0.5, Lith - Keizersveer v0.5

Authors

Willem Ottevanger, Victor Chavarrias, Marcela Busnelli, Amgad Omer, Carlijn Eijsberg

Cover: View of the Meuse River.

Morphodynamic model of the Meuse River

Linne - Roermond v0.5, Roermond - Belfeld v0.5, Belfeld - Sambeek v0.5, Grave - Lith v0.5, Lith - Keizersveer v0.5

Client	Rijkswaterstaat
Contact	Arjan Sieben, Roy Frings, Joey Ewals
Reference	SITO Programmasubsidie IenW 2024
Keywords	Meuse, Linne, Keizersveer, D-HYDRO, SMT, morphology

Document control

Version	1.0
Date	2024-07-22
Project number	11210364-002
Document ID	11210364-002-ZWS-0003
Pages	66
Status	final

Author(s)

	Willem Ottevanger	Deltares
--	-------------------	----------

Summary

The Meuse River at present does not have a validated numerical model for morphodynamics. To uniformise the approaches on the Rhine and the Meuse, a plan was developed for the construction of a two-dimensional morphodynamic model of the Meuse which builds on the recently developed hydrodynamic D-HYDRO model of the Meuse. Transition to D-HYDRO, is desired, since it is foreseen that the new hydrodynamic model will replace the current WAQUA hydrodynamic model in the future.

The hydrodynamic model includes the Meuse from Lixhe to Keizersveer. In 2021, a pilot reach in the Common Meuse (in Dutch: Gemeenschappelijke Maas, also Grensmaas) was identified near Meers. In past years, the location of Meers was modelled by carrying out multiple simulations. Also, the reach of Sambeek-Grave was selected as a second pilot location.

This document describes the preliminary construction of five submodels covering the following reaches of the River Meuse:

- i. Linne - Roermond v0.5
- ii. Roermond - Belfeld v0.5
- iii. Belfeld - Sambeek v0.5
- iv. Grave - Lith v0.5
- v. Lith - Keizersveer v0.5

At this early stage of model development for the five reaches, no calibration has been conducted yet. The initial outcomes are derived using the same morphological and sediment transport settings as employed in the pilot model of the Sambeek-Grave case study.

Hydrodynamic simulations were conducted using steady discharges for a schematized discharge hydrograph. From these simulations, the yearly sediment transport per kilometre was obtained and visually represented. These graphs demonstrate the initial sediment transport gradient, which dictates whether erosion or deposition will occur. Analyzing these graphs enables adjustments to be made to the input parameters — both hydraulic and morphological — to more accurately reflect the measured conditions.

Initial morphological computations covering a 4-year span (2014-2018) have been conducted. The temporal evolution of the bed level is visually presented, aiming at the assessment of input accuracy and model stability. However, these runs are not yet suitable for evaluating the model's accuracy as the model inputs require adaptation. These preliminary model results offer insights and recommendations for adjusting the model inputs, aimed at enhancing model stability, refining the initial sediment transport and its gradients, and improving the morphological outcomes.

Various challenges have emerged during the development of these submodels. This report addresses these challenges and provides recommendations for further development of these models.

Contents

	Summary	4
	List of Tables	7
	List of Figures	8
1	Introduction	10
1.1	Background and motivation	10
1.2	Objective	11
1.3	Current report	11
1.4	Outline	11
2	Approach for model setup	12
2.1	Background	12
2.2	Activities prior to 2023	12
2.3	Overview of the activities	13
3	Methodology	16
3.1	Hydrodynamic models	16
3.1.1	Maas hydrodynamic models	16
3.1.2	Boundary conditions submodels	17
3.1.3	Comparison submodels and entire model	17
3.1.4	Role of flood attenuation	17
3.2	Sediment transport models	18
3.2.1	Sediment properties	19
3.2.2	Sediment availability	20
3.2.3	Sediment transport formula	20
3.3	Morphological models	20
3.3.1	Hydrodynamic boundary conditions	21
3.3.2	Morphological factor	22
3.3.3	Initial bed level	23
3.3.4	Initial hydrodynamic conditions	23
3.3.5	Morphodynamic boundary conditions	23
4	Results	24
4.1	Linne-Roermond	25
4.1.1	Offline sediment transport	25
4.1.2	Morphological test 2014-2018	26
4.1.3	Outlook 2024	27
4.2	Roermond-Belfeld	28
4.2.1	Offline sediment transport	28
4.2.2	Morphological test 2014-2018	29
4.2.3	Outlook 2024	35
4.3	Belfeld-Sambeek	35
4.3.1	Offline sediment transport	35
4.3.2	Morphological test 2014-2018	37
4.3.3	Outlook 2024	44
4.4	Grave-Lith	44
4.4.1	Offline sediment transport	44
4.4.2	Morphological test 2014-2018	45
4.4.3	Outlook 2024	51
4.5	Lith-Keizersveer	51

4.5.1	Offline sediment transport	51
4.5.2	Morphological test 2014-2018	52
4.5.3	Outlook 2024	60
5	Conclusions and recommendations	61
6	References	64

List of Tables

2.1	Steps in model development	13
3.1	Overview of sediment fraction classes.	19
3.2	Preliminary choice for morphological factor per discharge.	22
5.1	Overview of model status and challenges	62
5.2	Overview of recommendations (outlook)	63

List of Figures

3.1	Q-Q relation for the standard dynamic simulations (Linne vs. Eijsden)	17
3.2	Q-Q relation for the standard dynamic simulations (Grave vs. Eijsden)	18
3.3	Approximation of discharges associated with different levels of the weirs opening (from ?)	19
3.4	Hydrograph for the period from 2014 to 2018	21
3.5	Step hydrograph applied for four years	22
4.1	Yearly sediment transport considering the standard parameters in the relation by Meyer-Peter and Müller (1948) and $ASKLHE=0.65$. The colours show the relative contribution of the different sediment fractions.	26
4.2	Bed level changes between $t=0$ and the peak discharge	27
4.3	Yearly sediment transport considering the standard parameters in the relation by Meyer-Peter and Müller (1948) and $ASKLHE=0.65$. The colours show the relative contribution of the different sediment fractions.	29
4.4	Bed level changes after 1 year (left) and after 4 years (right)	30
4.5	Initial bed levels in model and from measurements	31
4.6	Initial bed levels in the model	32
4.7	Average bed levels per river kilometre	33
4.8	Average bed level changes per river kilometre (bed level of indicated year minus initial bed level)	34
4.9	Incorrect velocity pattern at the downstream boundary	35
4.10	Weirs at the downstream boundary	36
4.11	Yearly sediment transport considering the standard parameters in the relation by Meyer-Peter and Müller (1948) and $ASKLHE=0.65$. The colours show the relative contribution of the different sediment fractions.	37
4.12	Bed level changes km 101 - km 112 after 1 year	38
4.13	Bed level changes km 113 - km 124 after 1 year	39
4.14	Bed level changes km 125 - km 136 after 1 year	40
4.15	Bed level changes km 137 - km 148 after 1 year	41
4.16	Initial bed levels in model and from measurements	42
4.17	Average bed levels per river kilometre after 1 year	42
4.18	Average bed level changes per river kilometre (Bed level year minus initial bed level)	43
4.19	Yearly sediment transport considering the standard parameters in the relation by Meyer-Peter and Müller (1948) and $ASKLHE=0.65$. The colours show the relative contribution of the different sediment fractions.	45
4.20	Bed level changes km 176 - km 186 after 1 year (left) and after 4 years (right)	46
4.21	Bed level changes km 187 - km 200 after 1 year (left) and after 4 years (right)	47
4.22	Initial Bed levels model and measurements	48
4.23	Average bed levels per river kilometre	49
4.24	Average bed level changes per river kilometre (bed level of indicated year minus initial bed level)	50
4.25	Yearly sediment transport considering the standard parameters in the relation by Meyer-Peter and Müller (1948) and $ASKLHE=0.65$. The colours show the relative contribution of the different sediment fractions.	52
4.26	Bed level changes km 201 - km 211 after 1 year (left) and after 4 years (right)	53
4.27	Bed level changes km 212 - km 224 after 1 year (left) and after 4 years (right)	54
4.28	Bed level changes km 225 - km 236 after 1 year (left) and after 4 years (right)	55
4.29	Bed level changes km 237 - km 248 after 1 year (left) and after 4 years (right)	56
4.30	Initial bed level in model and from measurements	57
4.31	Average bed levels per river kilometre	58

4.32 Average bed level changes per river kilometre (bed level of indicated year minus initial bed level)

59

1 Introduction

1.1 Background and motivation

The Meuse River, at present, does not have a validated two-dimensional numerical model for morphodynamics.

The current assessment of morphodynamic change can follow from:

- expert judgement
- WAQUA simulations in combination with the offline post-processing tools WAQMORF
- Ongoing development of a similar tool for D-HYDRO called D-FAST Morphological Impact.
- The large scale 1D model by [Berends *et al.* \(2020\)](#).

The above analyses offer order-of-magnitude values, and are restricted to a single measure. When considering system-wide measures an up-to-date morphodynamic model is needed for river management issues such as:

- project design of interventions in or along the main channel of “summer bed” (removal of bed and bank protection, sediment management),
- impact assessment for evaluation of measures (river engineering assessment framework and licensing),
- analyses of monitoring in pilots (sediment management, eroding banks, river width adjustment such as by longitudinal training walls, etc.),
- system analyses for long-term scenarios with management variants, e.g. for IRM (Integraal RivierManagement – Integrated River Management) so that estimates can be made of the effects of the morphological development on the different river functions.

To align the approaches on the Rhine and the Meuse, a plan was developed for the construction of a two-dimensional morphodynamic model of the Meuse which builds forward on the recently developed hydrodynamic D-HYDRO model of the Meuse ([De Jong, 2021](#)). This development is ongoing for the Rhine model as well.

Development of the morphodynamic model using D-HYDRO is desired, since it is foreseen that the new sixth generation hydrodynamic model ([De Jong, 2021](#)) will soon replace the current fifth generation WAQUA hydrodynamic model. It therefore makes sense to align the software for the morphodynamics as well.

1.2 Objective

The objective of this project is the development of a new modelling instrument that simulates the complex spatial riverbed dynamics in the Meuse river, enabling us to predict developments and effects of interventions in the riverbed, examine options for long-term (2050-2100) management and policy decisions, and thus shape the river management of the future.

1.3 Current report

This document describes the preliminary construction of five submodels covering the following reaches of the River Meuse:

- i. Linne - Roermond v0.5
- ii. Roermond - Belfeld v0.5
- iii. Belfeld - Sambeek v0.5
- iv. Grave - Lith v0.5
- v. Lith - Keizersveer v0.5

The primary objective of this document is to describe the current state of the developed Meuse submodels within the five reaches. The pilot case study between Sambeek and Grave is described in a separate report (?).

Various challenges have emerged during the development of these submodels. This report addresses these challenges and aims to provide recommendations for furthering development of these models.

1.4 Outline

The document is organized as follows. Chapter 3 explains the methodology. The methodology consists of three steps: hydrodynamic models (Section 3.1), sediment transport models (Section 3.2), and morphodynamic models (Section 3.3). Chapter 4 describes the preliminary results per submodel. Chapter 5 presents the main conclusions and recommendations.

2 Approach for model setup

Spruyt and Ottevanger (2019) developed a plan of action for the development of the morphological model for the Meuse. Based on this, they present a general approach, which foresees a model development in several steps. These steps are extended as follows for this project:

- v0 This version is a basic model that contains the most important functionality, with the main goal to have a running but not yet too complex model.
- v1 Building on v0, the first model version is a version which covers similar functionality as is provided for the Rhine by the existing DVR (Duurzame Vaardiepte Rijndelta) model. Moreover, the model is based on the latest available data and insights.
- v2 The second model version is based on v1 but extended with new functionality to make the model suitable for more types of applications (e.g. finer grids, exchange of sediment between main channel and flood plains, bank erosion processes, etc.).
- v3 The third model version is used to develop new insights and functionality.

Table 2.1 shows the development of the model according to the different phases and an overview of the progress in the past years.

2.1 Background

The hydrodynamic model set up by De Jong (2021) includes the Meuse from Lixhe to Keizersveer. Different weir operations are incorporated in the model. Moreover to calibrate the model different model versions have been setup. These represent the river geometry in the years 1995, 2012, 2014 and 2019. In these years, different floods occurred which enable the validation for the high-discharge events.

2.2 Activities prior to 2023

An initial model was set up by Ottevanger *et al.* (2020).

In 2021, a pilot reach in the Common Meuse (in Dutch: Gemeenschappelijke Maas, also Grensmaas) was identified near Meers. The location of Meers was modelled by carrying out multiple simulations. The current status of the Meers model is that there are still differences in the results between sequential and parallel runs. Although many runs were performed and different software bugs were resolved, the differences remain at this location. It is hypothesized that the inherent sensitivity of the system (geometry, mathematical formulations and the numerical translation thereof) lead to differences which can be large with respect to an initial perturbation.

Since 2022, the reach of Sambeek-Grave was selected as a second pilot location. This location is well suited as there is a large-scale measure (summer-bed lowering) which has been implemented and the bed level is measured every year. Moreover, the reach has a lower slope and it appears that models of low-slope rivers are found to be less sensitive, compared to the steeper river reaches like the Meers model. This is demonstrated by findings in a model of the Western Scheldt and different schematic river models.

2.3 Overview of the activities

Table 2.1 describes the model development steps per sub-category, and the present status of the different reaches of the Meuse. For legibility the following abbreviations have been introduced:

- EK: Eijsden-Keizersveer,
- LiK: Lixhe-Keizersveer,
- ML: Monsin-Lixhe,
- LB: Lixhe-Borgharen,
- BL: Borharen-Linne,
- LR: Linne-Roermond,
- RB: Roermond-Belfeld,
- BS: Belfeld-Sambeek,
- SG: Sambeek-Grave,
- GL: Grave-Lith,
- LK: Lith-Keizersveer.

Table 2.1 Steps in model development

activity areas	associated activities	model version	2020	2021	2022	2023
data collection	• Collection of all data needed to set up a model, e.g. boundary conditions, calibration data hydrodynamics and sediment transport and morphology, bed composition, etc.	v0,v1	EK - v0, Meers - v0	SG	SG, Li-K	SG v0.8, LR v0.5, RB v0.5, BS v0.5, GL v0.5, LK v0.5
morphodynamic model schematization: towards a well-working basic model (v0)	• set-up of a first running model including: a. dynamic river bed b. representative initial bed elevation (e.g. smoothing of bed forms) c. suitable roughness formulation for morphology d. sediment (grain sizes and sediment layers, with focus on active/upper layer) e. secondary flow f. first choice of transport formula and parameters (uncalibrated)	v0		SG SG - v0.5 EK		SG

(continues on next page)

Table 2.1 – continues from previous page

activity areas	associated activities	model version	2020	2021	2022	2023	
	<p>g. non-erodible and less erodible layers</p> <p>h. suitable grid resolution</p> <ul style="list-style-type: none"> • testing phase v0 model, identification of problems and modification of the schematization accordingly 			EK	SG - lokale 20 m	LR, RB, BS, GL, LK - 20 m	
extending the basic model to a v1 model	<ul style="list-style-type: none"> • more sophisticated description of <ul style="list-style-type: none"> a. main channel roughness b. composition and thickness of underlayers, including non-erodible layers • set-up of a dredging and dumping module • testing phase v1 model, and iterative modification of model schematization if necessary 	v1			SG	(sed.trans. including separate roughness) SG (fully mobile)	
development of methodologies and tools for running the model	<ul style="list-style-type: none"> • approach and tools for model simulation (i.e. Simulation Management Tool) • strategy for model spin-up • strategy and tools for model evaluation and presentation of results • strategy and tools for simplification of model set-up and improving reproducibility 	v0,v1	EK, EK - v0		SG - Too coarse	SG - Local 20 m	<p>Improvement of restart to seconds</p> <p>Submodels based on standard simulations</p> <p>Start on user manual</p>
model calibration and validation	<ul style="list-style-type: none"> • calibration and validation strategy • adapting the hydrodynamic model to make it suitable for morphodynamic simulations • hydrodynamic validation • <i>offline</i> calibration giving a first estimate of morphological response based on the flow field in the hydrodynamic simulations • 1D morphodynamic calibration and validation (focusing on width-averaged, large-scale and long-term trends) 	v1			2014-2018	<p>2014-2018 remove weirs</p> <p>50000 m³/year, Influence of fixed layers</p>	<p>2014-2018 20 m sub-models</p> <p>SG v0.8, LR v0.5, RB v0.5, BS v0.5, GL v0.5, LK v0.5</p> <p>Jump at SG lowering Analysis of statistical output of bed level changes</p>

(continues on next page)

Table 2.1 – continues from previous page

activity areas	associated activities	model version	2020	2021	2022	2023
	<ul style="list-style-type: none"> • 2D morphodynamic calibration and validation (focusing on 2D patterns in the river bed, such as bar patterns and bend profiles) • validation of dredging and dumping module 					
exploring model uncertainties	<ul style="list-style-type: none"> • influence of unknown physical variables (e.g. roughness in transport, bed composition, active layer thickness) • influence of model settings (e.g. initial geometry/composition and boundary conditions) or modelling concepts (e.g. Hirano model) • influence of simulation strategy and approaches (e.g. methods for optimizing simulation time, schematization of the hydrograph, choice of simulation period) 	v1-v3				
development of modelling strategies and development for future use of the model	<ul style="list-style-type: none"> • identifying types of application and requirements • development of strategies for application of the model (e.g. choice of scenarios, choices • for model settings and geometry, type of interventions) • identifying needs for further development of the model schematization (including needs for knowledge development and data requirements) • implementation and testing 	v1-v3				
verification of model application	<ul style="list-style-type: none"> • testing the model application in test cases of <ol style="list-style-type: none"> a. effect of interventions b. planning study (<i>planstudie</i>) c. (long-term) forecast of system behaviour • improvement of the model schematization, modelling strategies, methodologies and tools based on the outcomes of the test cases 	v1-v3				
implementation of new functionality in D-HYDRO	<ul style="list-style-type: none"> • identifying requirements of new functionality • functional design of needs • design of implementation • implementation and testing • updating user manuals 	v2-v3				
reports			Ottevanger <i>et al.</i> (2020)	Ottevanger <i>et al.</i> (2021); Ottevanger (2021a)	Ottevanger and Chavarrias (2022b,a)	Ottevanger <i>et al.</i> (2024); ?
related work				Chavarrias (2021)	Chavarrias and Ottevanger (2022)	

3 Methodology

The submodels for the five reaches of the River Meuse are developed in stages. Initially, the hydrodynamic models are constructed, followed by the sediment transport models (excluding alterations in bed level and sediment composition), and finally, the morphological models are established.

The hydrodynamic models for the entire River Meuse have been previously constructed (De Jong, 2021). However, their primary focus lies in accurately reproducing measured water levels. As a result, they have been predominantly adapted based on the experience gained from the morphological models and the new insights obtained from the SambEEK-Grave morphological modelling pilot study by Ottevanger and Chavarrias (2022a).

3.1 Hydrodynamic models

Hydrodynamic models for the five reaches have been developed based on the Baseline schematization from both the years 2023 and 2014. Although a 20 m grid is necessary to define the main channel and is applied for the morphological simulations, a 40 m grid has been used in the hydrodynamic simulations. This decision was made because a model with a larger grid size runs faster, and the hydrodynamic results do not significantly differ. Consequently, it became possible to test and generate boundary conditions for the submodels using a 20 m grid from the hydrodynamic run of the whole 40 m grid model. The process involved the following steps for the j14 and j23 schematizations:

- i) Running the entire Maas hydrodynamic models with a 40 m grid for different discharge conditions: 50, 125, 259, 500, 750, 1000, 1300, 1700, 2100, 2500, 2800 and 3200 m³/s.
- ii) Creating the submodel grids by cutting the complete grids (SI20m and 40 m) and establishing boundary conditions per cell from the results of the whole model (40 m grid) per discharge.
- iii) Verifying the hydrodynamic model results by comparing the outcomes between the whole model and the submodels utilizing the 40 m grid.

3.1.1 Maas hydrodynamic models

The initial hydrodynamic and sediment transport computations are based on the BASELINE schematisation j14-6-w14a. There is also a schematisation of 2023 (j23-6-v1a) available and it has been applied to create the hydrodynamic and sediment transport models, however this will not be reported in the current document. This is important for future applications of the model, related to a near current schematisation.

There are two grids: the 40 m grid and the 20 m grid. The 40 m grid consists of only one hydrodynamic model of the entire Maas. However, with the 20 m grid, there are three submodels of the Maas.

3.1.2 Boundary conditions submodels

The most optimal results were achieved by implementing boundary conditions per grid cell. These boundaries were derived from the model results of the entire 40 m grid model. At the upstream boundary, a discharge condition per cell is set, while downstream, a water level condition per cell is applied. These conditions yield favorable results when comparing the outcomes of the entire model with the submodels.

3.1.3 Comparison submodels and entire model

Visual comparisons were made between the water level and velocity fields simulated by the submodels and those generated by the entire Maas model. These comparisons also extended to contrasting the submodel results with the outcomes derived from the two grids, highlighting a consistency in water levels and velocity fields across all models.

3.1.4 Role of flood attenuation

For application of the morphological model, different stationary discharges were used. The discharges were chosen to align with the currently available stationary simulations in the Meuse. This route was chosen, because the boundary conditions are readily available for the 40 m models.

An investigation into the discharge propagation along the Meuse was performed using the dynamic discharge simulations (D1300, D1700, D2100, D2500, D2800, D3200, D3600) including extra output at the weirs (which form the boundaries of the submodels), showing that the effect of flood attenuation was largely compensated for by the lateral input of side channels and tributaries, after the peaks of the flood were shifted to align. [Figure 3.1](#) and [Figure 3.2](#) show the comparison at Linne and Grave.

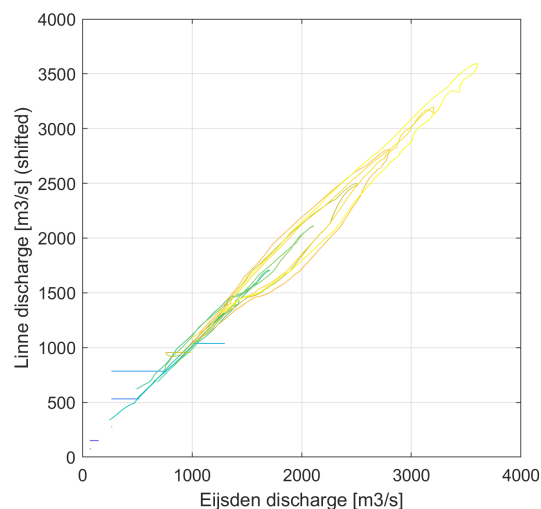


Figure 3.1 Q-Q relation for the standard dynamic simulations (Linne vs. Eijsden)

Based on this observation, we conclude that for the standard simulations, using the Eijsden discharge for each of the submodels is a reasonable first approximation. It should be mentioned, however that the stationary simulations also include the effect of lateral inflows, which implies that the discharge in the downstream reaches will increase compared to the imposed discharge at Eijsden. To compensate for this in the stationary simulations, full model simulations with reduced discharges at the upstream boundary should be derived. This approach can also be used for hindcasts in which the role of flood attenuation could be significant (e.g. in the flood wave of 2021).

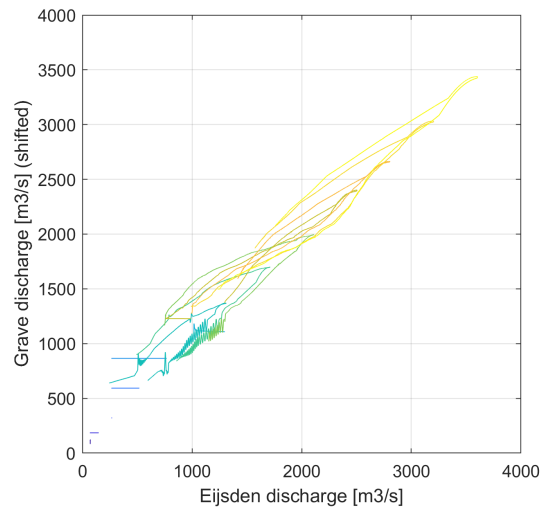


Figure 3.2 Q-Q relation for the standard dynamic simulations (Grave vs. Eijsden)

The choice of the stationary discharges should also be evaluated. Currently the available discharges were used. However, based on considerations of when certain parts of the river start to flow could be used as boundaries for categories of different discharge regimes. [Sieben \(2023\)](#) proposes to use 50, 1250, 2300 as boundaries, which results in four categories of discharges:

- $<50 \text{ m}^3/\text{s}$ main channel only, with closed weirs
- $50 \text{ m}^3/\text{s} < 1250 \text{ m}^3/\text{s}$ main channel only, weirs opening
- $1250 \text{ m}^3/\text{s} < 2300 \text{ m}^3/\text{s}$ developing flow through winterbed, with open weirs
- $>2300 \text{ m}^3/\text{s}$ fully developed flow through winterbed, with open weirs

Based on these categories and possibly some extra to account for weir operation (cf. [Figure 3.3](#)), new representative discharges can be derived. When performing a hindcast, even effects of flood attenuation could be derived for different reaches.

3.2 Sediment transport models

Sediment input files have been generated for the five reaches using a 20 m grid, and sediment transport models (without accounting for bed level changes) have been developed for the schematic years 2023 and 2014 in the five submodels.

The input required to define these models are:

- i) Sediment properties: sediment types with particle diameters and densities.
- ii) Sediment availability: number of layers and sediment-layer thickness.
- iii) Sediment transport formula: type of empirical sediment transport formula for each sediment type.

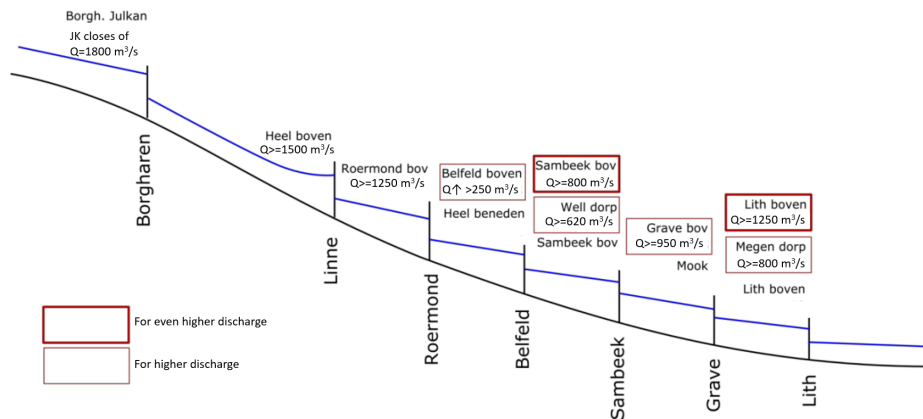


Figure 3.3 Approximation of discharges associated with different levels of the weirs opening (from ?)

3.2.1 Sediment properties

The sediment information was compiled in the model by Berends *et al.* (2020) based on earlier work by Sloff and Barneveld (1996); Sloff and Stolker (2000); Berkhout (2003). Frings (2022) has updated the sediment properties of the old measurement campaign and the new measurements. The analysis by Frings (2022) describes the top layer content and the 10 km moving-average along the channel.

The sediment classes have been updated based on this analysis, incorporating subsurface layers as used in the model by Berends *et al.* (2020), which are imposed where the sand-gravel boundary of 2 mm was added to the sand classes (cf. Table 3.1).

In total there 11 sediment fractions: 4 are sand particles and 7 are gravel.

Sediment fraction	Minimum diameter [m]	Maximum diameter [m]
Sediment1	8.00e-05	1.25e-04
Sediment2	1.25e-04	2.50e-04
Sediment3	2.50e-04	1.00e-03
Sediment4	1.00e-03	2.00e-03
Sediment5	2.00e-03	4.00e-03
Sediment6	4.00e-03	8.00e-03
Sediment7	8.00e-03	1.60e-02
Sediment8	1.60e-02	3.15e-02
Sediment9	3.15e-02	6.30e-02
Sediment10	6.30e-02	1.00e-01
Sediment11	1.00e-01	2.00e-01

Table 3.1 Overview of sediment fraction classes.

3.2.2 Sediment availability

Ottevanger (2021b) analysed the bed level variation in 2018, 2019 and 2020 and combined this with known locations of fixed layers. This information was used to prescribe the sediment availability in the model. It was assumed that there is 8 m of available sediment in general matching the value as used by Berends *et al.* (2020). At bank zones the initial sediment thickness is assumed to be zero, thereby matching the current approach in the DVR models. At locations which exhibit limited changes (cf. Ottevanger *et al.*, 2021) for the initial runs a thickness of 8 m is imposed. In the Sambeek-Grave reach this approach gave good results for the infilling of the summerbed lowering (cf. ?). Nevertheless, the option to adjust these regions may still be necessary on other reaches of the Meuse.

The sediment under-layers are imposed starting at the current bed level as the zero reference. As indicated by ? in the study of Sambeek-Grave, there may have been significant bed level degradation since the original data. It is a good point to investigate the effect of this choice in the model. This is also left as a recommendation for further research.

3.2.3 Sediment transport formula

The model applies the general formula which has the structure of the Meyer-Peter-Mueller formula (Meyer-Peter and Müller, 1948) but all coefficients can be adjusted. The same coefficients as Meyer-Peter and Müller (1948) except for the critical mobility parameter are applied for all the fractions. The critical parameter is taken 0.025 instead of 0.047 as applied in the Sambeek-Grave model.

The model also incorporates a hiding-exposure correction for the critical shear stress of the different particles, adopted from the Sambeek-Grave model (?).

3.3 Morphological models

Morphological submodels for the five reaches are created using the Simulation Management Tool (SMT). Within the SMT, a hydrograph is discretized into a series of constant (steady) discharges, enabling the application of various morphodynamic factors per discharge. However, this approach cannot model the dynamics of a flood wave. Unlike the varying peak discharge at different locations along a river during a flood wave, the discharge for each step in the schematized hydrograph remains constant throughout the entire domain when using the SMT. This means that flood wave attenuation, which causes varying peak discharges during a flood wave, is not accounted for.

The acceptability of the SMT results relies on the assumption of negligible flood wave attenuation. This assumption might seem less acceptable in longer domains or steeper hydrographs, but has been demonstrated to remain valid for a large range of such conditions (Barneveld *et al.*, 2024). To assess its applicability to our specific case, the hydrodynamic effects of flood waves in comparison with steady discharges have been studied. From this analysis it is concluded that applying steady discharges to the morphodynamic model of the River Meuse is acceptable.

The model first underwent calibration and validation using measurements. For this purpose, the Baseline schematisation j14_6-w14a from the year 2014 was utilized.

To define the SMT for the morphological submodels, the following input is required:

- i Hydrodynamic boundary conditions: The upstream hydrograph is defined by constant discharges as a function of time, representing a specific period.
- ii Morphological factor: These factors are defined for each discharge.
- iii Initial bed level: The bed levels at grid cell-centers need to be defined.
- iv Initial hydrodynamic conditions: Steady conditions are established for every discharge in the step hydrograph.
- v Morphodynamic boundary conditions: These encompass bed level changes and need to be defined.

3.3.1 Hydrodynamic boundary conditions

The upstream boundary condition is established as a series of constant discharges. To achieve this, the discharges measured from 2014 to 2018, as detailed by ?, have been analyzed. Figure 3.4 shows the discharge measurements.

Subsequently a schematic discharge wave is created for use with the simulation management tool (SMT, cf. *Yossef et al., 2008*; *Ottevanger et al., 2020*). The approach used is similar to *Yossef et al. (2008)*, in which the hydrograph is modelled through a set of constant-discharge simulations with varying morphological factor, rather than a dynamic hydrograph. Figure 3.5 depicts the schematized step hydrograph.

The discharge boundary conditions at the upstream boundary and the water levels at the downstream boundary per cell have been acquired, as detailed in Section 3.1.2.

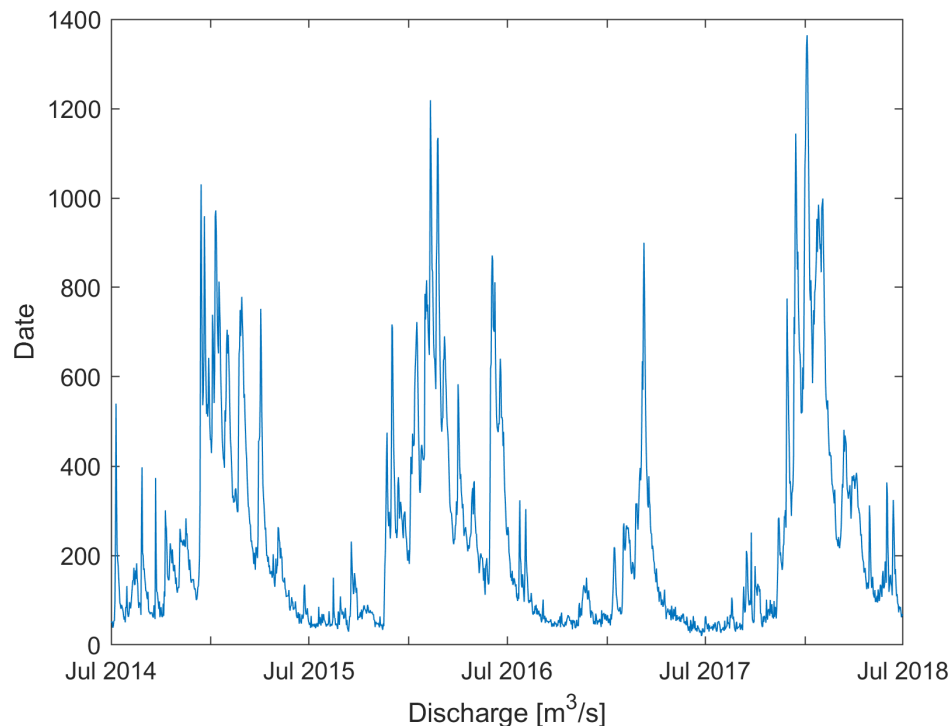


Figure 3.4 Hydrograph for the period from 2014 to 2018

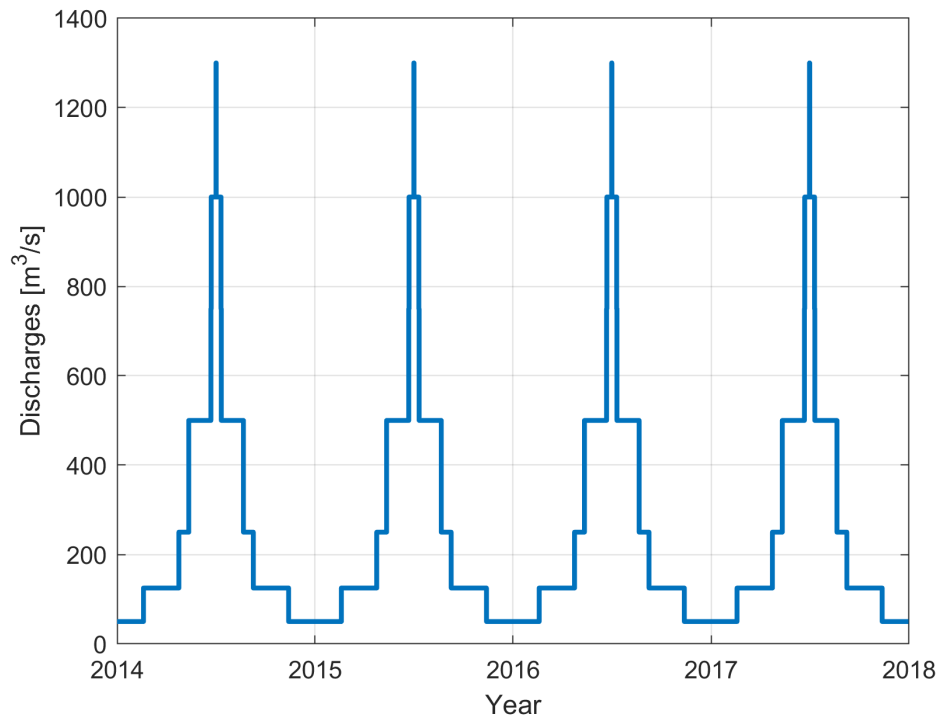


Figure 3.5 Step hydrograph applied for four years

3.3.2 Morphological factor

The SMT approach allows a strong reduction in the computational time. As different morphological acceleration factors can be used, depending on the discharge, the actual time needed to compute the bed level development can be significantly reduced. Table 3.2 shows an initial overview of the imposed morphological factors, which could still be subject to change in the future.

For the 50 m³/s discharge level the morphological factor is much higher than for the other discharges, but there is no composition or bed update during this time. It has been included to ensure that the morphological time frame is easier to process. During the low flow period the bed level changes are considered to be small, and therefore a larger MORFAC can be used. At the peak discharges a smaller MORFAC is used.

Discharge [m ³ /s]	MORFAC
50	1440
125	40
250	40
500	40
750	10
1000	5
1300	1

Table 3.2 Preliminary choice for morphological factor per discharge.

3.3.3 Initial bed level

The initial bed level for the Baseline schematization j14_6-w141a from the year 2014 was extracted from the grid file generated with Baseline. Bed level sample files (.xyz) at centre points were created as required for morphological simulations.

3.3.4 Initial hydrodynamic conditions

It is crucial to initiate the morphological computations with a hydrodynamic initial condition that has attained the steady-state solution for every discharge to be simulated in the time series. Hence, hydrodynamic simulations (without updating the bed level and sediment composition) are initially conducted with a constant value for each discharge, allowing enough time to achieve a steady-state. This was confirmed by plotting time series of cross-section discharges, water levels, and velocities at both the upstream and downstream model locations. Additionally, 2D patterns at different times were visually compared.

3.3.5 Morphodynamic boundary conditions

The default boundary conditions have been initially applied, involving equilibrium sediment transport at both boundaries. Further model adaptations and evaluations are necessary in this context.

4 Results

This chapter presents the preliminary model results for the five submodels of the River Maas. At this early stage of model development, no calibration has been conducted yet. The initial outcomes are derived using the same morphological and sediment transport settings as employed in the pilot model of the Sambeek-Grave case study. However, variations exist in the implemented hydrodynamical and morphological boundaries across the five submodels when compared to the Sambeek-Grave model.

As outlined in Chapter 3, each cell in the newly developed models incorporates a specific boundary condition derived from results obtained in hydrodynamic model runs across the entire River Meuse model. The boundary conditions for the Sambeek-Grave model were established based on measured discharges and water levels. In the submodels, the morphological boundary conditions are based on default settings, assuming equilibrium in sediment transport upstream. Contrastingly, for the Sambeek-Grave model, an erosion of 5 cm/year has been applied at the upstream boundary. Further elaboration on these hydrodynamic and morphological settings is provided in Chapter 3.

The following sections present the preliminary model results for each submodel, categorized into three subsections: Offline sediment transport, Model test 2014-2018, and Outlook 2024.

Offline sediment transport

Hydrodynamic simulations were conducted using steady discharges for the discharge hydrograph shown in Figure 3.5. From these simulations, the yearly sediment transport per kilometre was obtained and visually represented. These graphs demonstrate the initial sediment transport gradient, which dictates whether erosion or deposition will occur. Analyzing these graphs enables adjustments to be made to the input parameters — both hydraulic and morphological — to more accurately reflect the measured conditions.

Morphological test 2014-2018

Initial morphological computations covering a 4-year span have been conducted, employing the same discharge hydrograph (Figure 3.5) and the bed level from the year 2014. The temporal evolution of the bed level is visually presented, aiming at the assessment of input accuracy and model stability. However, these runs are not yet suitable for evaluating the model's accuracy as the model inputs may require adaptation based on these preliminary hydrodynamic and morphological results.

Outlook 2024

These preliminary results offer insights and recommendations for adjusting the model inputs, aimed at enhancing model stability, refining the initial sediment transport and its gradients, and improving the morphological outcomes.

4.1 Linne-Roermond

4.1.1 Offline sediment transport

Using a model with a fixed bed an estimate for the sediment transport is derived. The Meyer-Peter and Müller (1948) formula and settings, including a hiding-exposure correction for the critical shear stress of the different particles. This model is based on the actual river information as known in 2014 (j14). By combining different steady-state discharge simulations and the frequency of occurrence of discharges as found for the period between 2014 and 2018, a total transport per year is calculated. The average data inside the polygon of the main channel is used to compute the sediment transport rate.

Figure 4.1 depicts the calculated annual sediment transport based on the step hydrograph (Figure 3.5).

The sediment transport at the upstream boundary is nearly eight times higher than one kilometre downstream. Due to the weirs at Linne, local velocities significantly increase. Because of the weir and local bed protection, erosion is unlikely to occur. However, transported material will deposit due to reduced sediment transport capacity from the start to kilometre 72. Between kilometres 72 and 73, as well as between kilometres 76 and 78, there is an increase in sediment transport, allowing erosion. Conversely, between kilometres 73 and 76, and from kilometre 78 to the end, there is a decrease in sediment transport, leading to sedimentation.

An analysis must verify the plausibility of the patterns of these sediment transport gradients and absolute values. This process begins with examining the hydrodynamic parameters, as changes in velocities significantly influence sediment transport. Subsequently, the analysis encompasses sediment transport and morphological parameters.

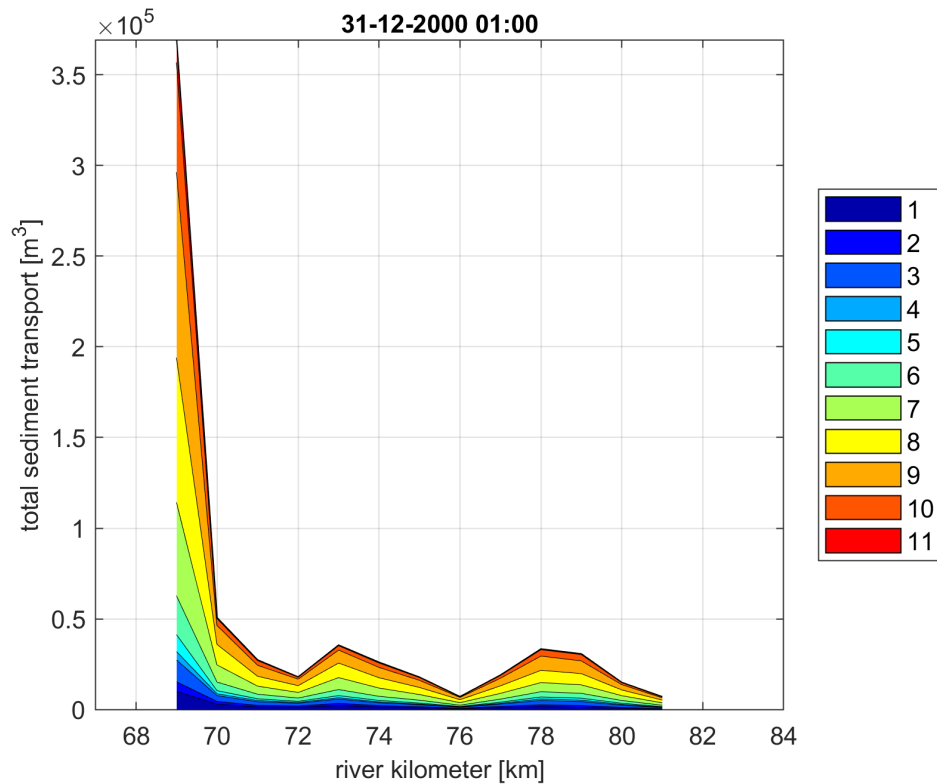


Figure 4.1 Yearly sediment transport considering the standard parameters in the relation by Meyer-Peter and Müller (1948) and ASKLHE=0.65. The colours show the relative contribution of the different sediment fractions.

4.1.2 Morphological test 2014-2018

The bed level developments (Figure 4.2) indicate unrealistic sedimentation upstream right from the beginning of the simulation, leading to the main termination of the simulation. This aligns with the negative sediment transport gradient (Figure 4.1). Consequently, a thorough reevaluation of both hydraulic and morphological upstream boundary conditions is necessary to enhance the model's performance. Additionally, the sediment availability in this section necessitates adjustments within the model.

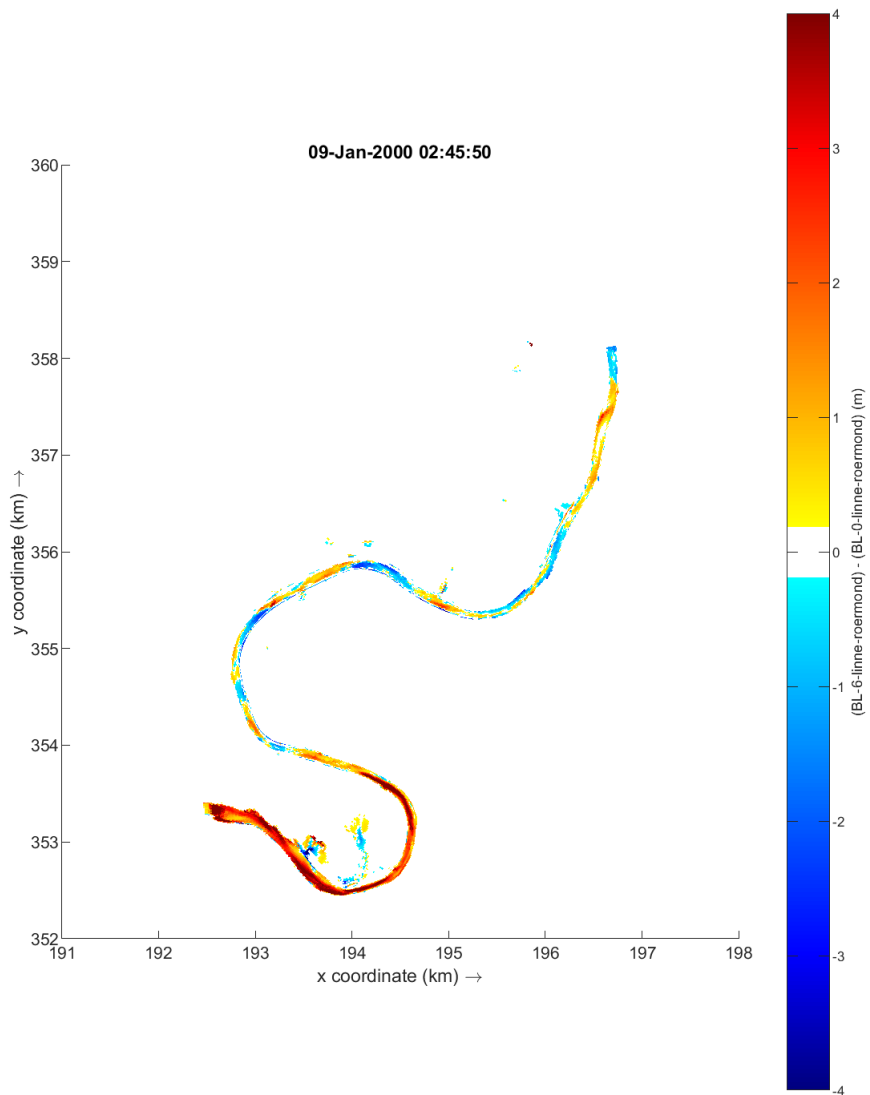


Figure 4.2 Bed level changes between t=0 and the peak discharge

4.1.3 Outlook 2024

The model tests have yielded valuable insights into enhancing the morphological simulations. It is imperative to verify and enhance both hydrodynamic and morphological boundary conditions. This might necessitate slight adjustments to the model's extent, particularly considering that boundaries were initially placed precisely at the locations of the weirs. Once these improvements have been made, our next step will involve identifying additional areas where realistic bed developments are not represented accurately. This will involve incorporating measurements into our analyses. Furthermore, expanding the simulation to encompass different time periods will be essential for comparison and validation.

4.2 Roermond-Belfeld

4.2.1 Offline sediment transport

Using a model with a fixed bed an estimate for the sediment transport is derived. The Meyer-Peter and Müller (1948) formula and settings, including a hiding-exposure correction for the critical shear stress of the different particles. This model is based on the actual river information as known in 2014 (j14). By combining different steady-state discharge simulations and the frequency of occurrence of discharges as found for the period between 2014 and 2018, a total transport per year is calculated. The average data inside the polygon of the main channel is used to compute the sediment transport rate.

Figure 4.3 depicts the calculated annual sediment transport based on the step hydrograph (Figure 3.5).

The sediment transport displays abrupt changes, both increasing (from km 81 to km 85 and from km 90 to km 96) and decreasing (from km 85 to km 90 and from km 100 to km 101), with relative stability observed between km 96 and km 100. These varying gradients in sediment transport—both positive and negative—will lead to significant alterations in erosion and sedimentation patterns, depending upon the composition of the bed.

An analysis must be conducted to verify the plausibility of these sediment gradient patterns and absolute values. These analyses involve not only analysis of the sediment parameters but also hydrodynamics, as changes in velocities significantly influence sediment transport.

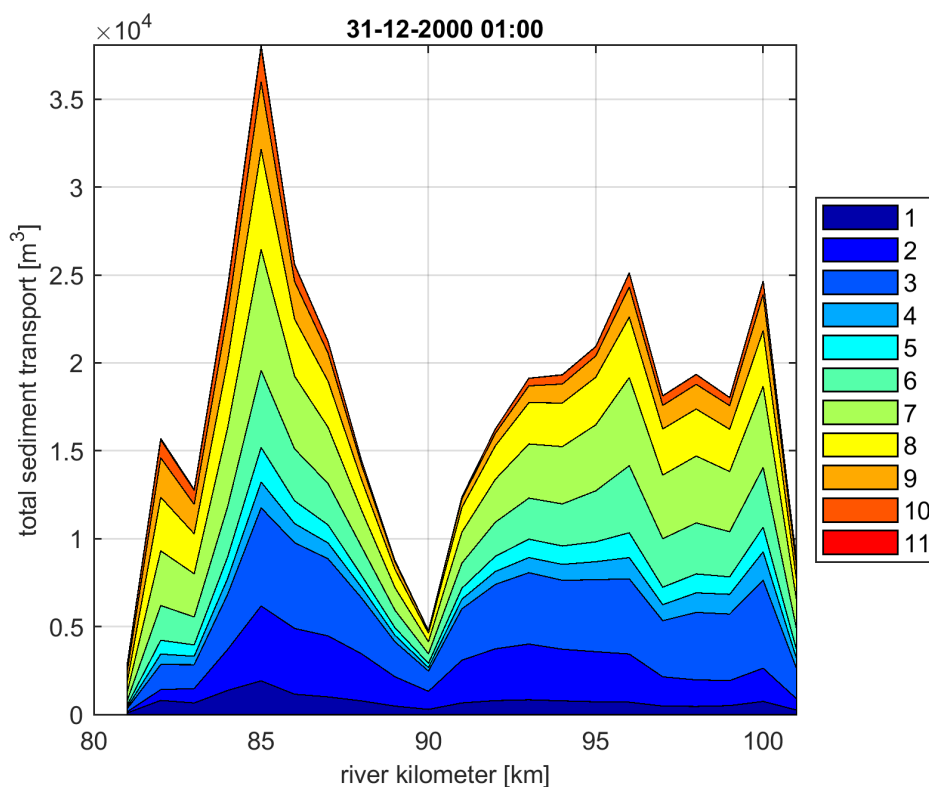


Figure 4.3 Yearly sediment transport considering the standard parameters in the relation by Meyer-Peter and Müller (1948) and ASKLHE=0.65. The colours show the relative contribution of the different sediment fractions.

4.2.2 Morphological test 2014-2018

In alignment with the sediment transport gradients shown in Figure 4.3, the alterations in bed level after the first simulation year (left plots in Figure 4.4) and after 4 years (right plots in the same figure) indicate potentially unrealistic values for erosion and sedimentation within this reach. Consequently, a comprehensive analysis of the hydraulic, sediment, and morphological parameters needs to be conducted. Nonetheless, the model has operated without stability issues throughout the entire 4-year period.

To assess the realism of the model results, the bed level developments in the model are compared with the measurements. The average initial bed levels measured per river kilometre are compared to those applied in the model. As shown in Figure 4.5, notable differences exist between these bed levels. Particularly, a significant depth is observed at the start of the reach in the model (Figure 4.6). Therefore, a closer examination is necessary to understand the disparities between the measurements and the initial bed levels in the morphological models.

The computed bed levels using the model for 1, 2, 3, and 4 years are depicted in Figure 4.7 alongside the corresponding measured bed levels. Additionally, Figure 4.8 illustrates the bed level changes after 1, 2, 3, and 4 years (bed level year minus initial bed level). As evident from these figures, the model computes unrealistic bed level changes. These differences arise from variations in the initial conditions and substantial positive and negative sediment transport gradients.

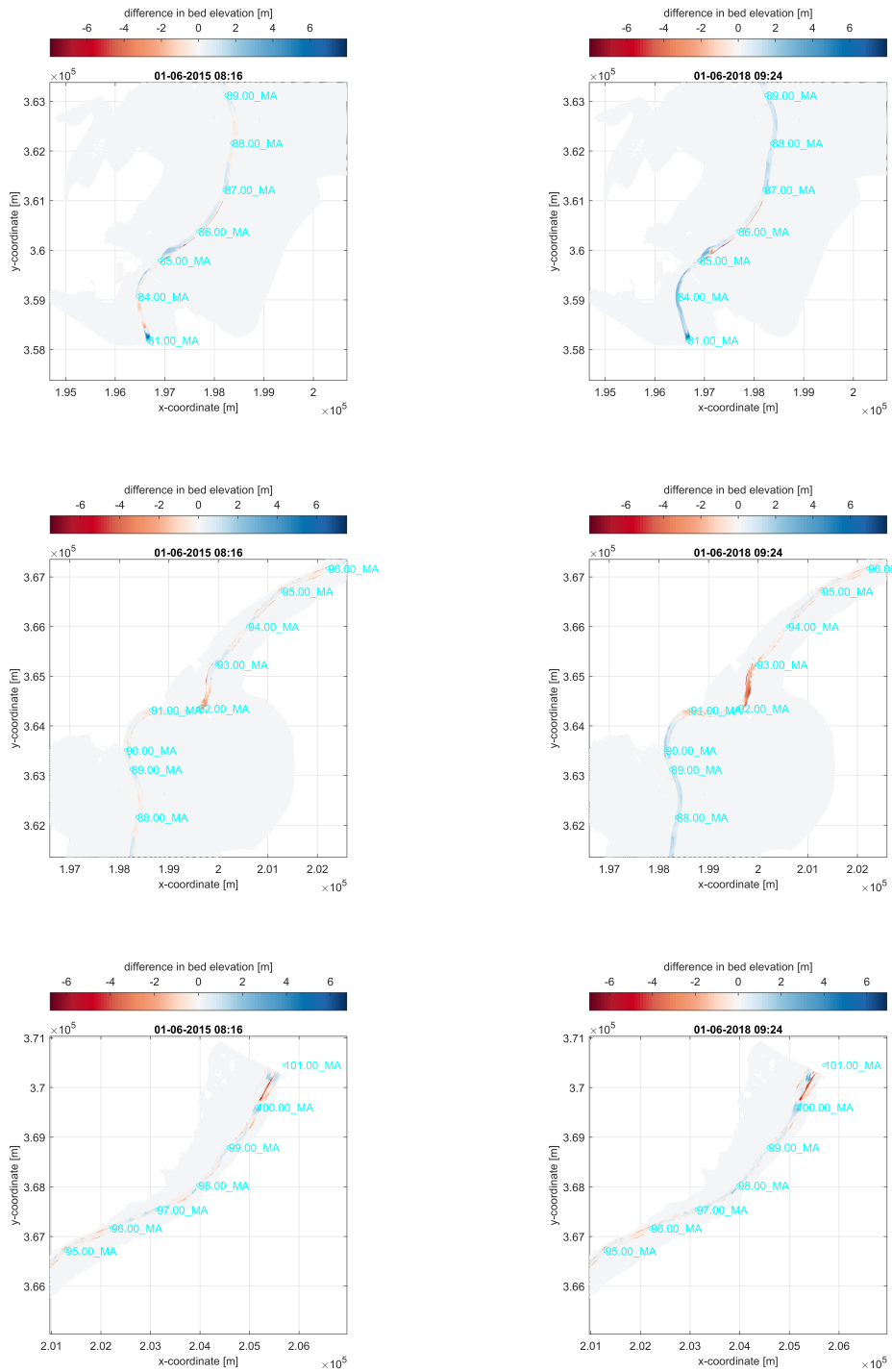


Figure 4.4 Bed level changes after 1 year (left) and after 4 years (right)

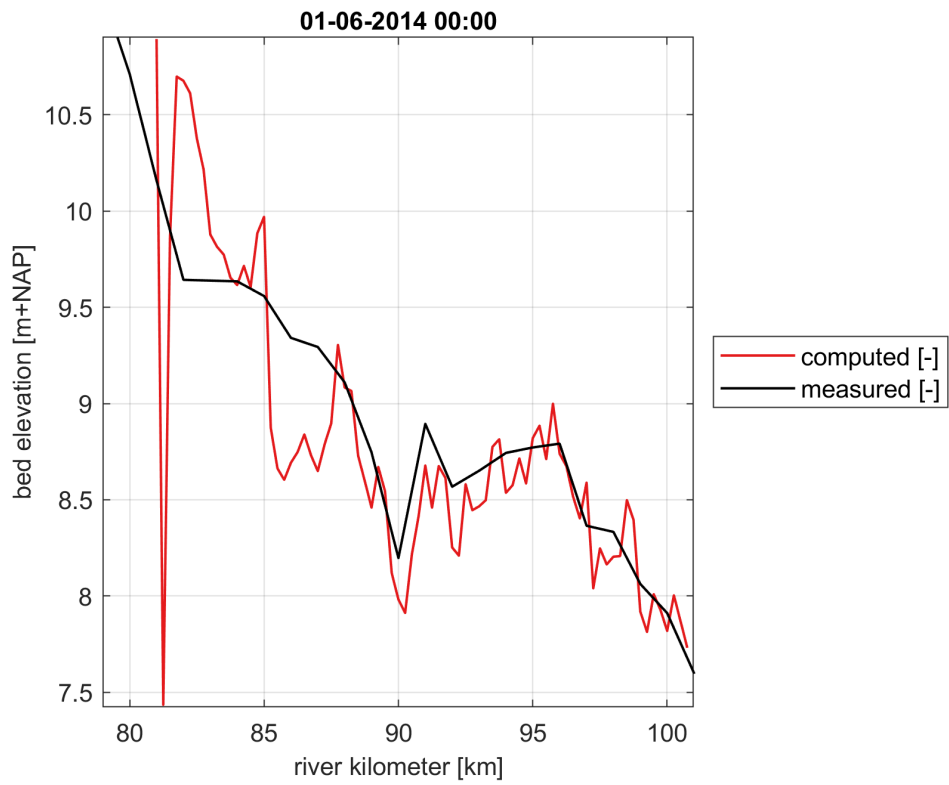


Figure 4.5 Initial bed levels in model and from measurements

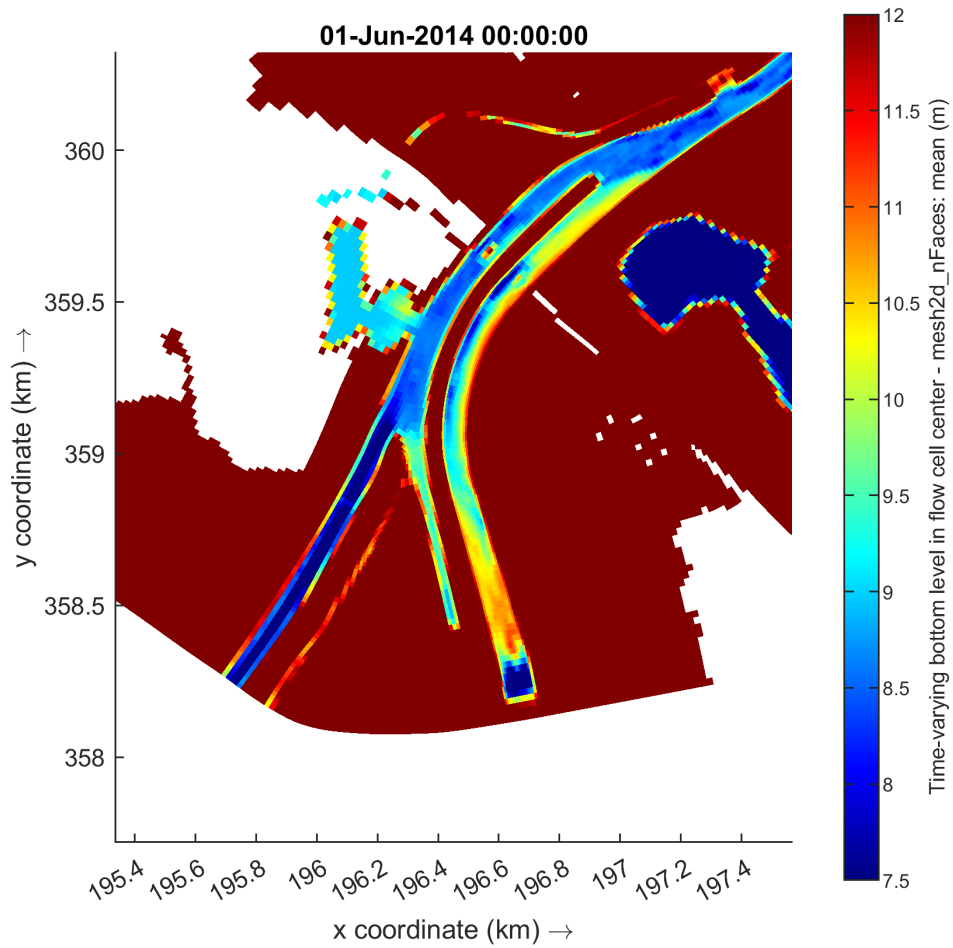
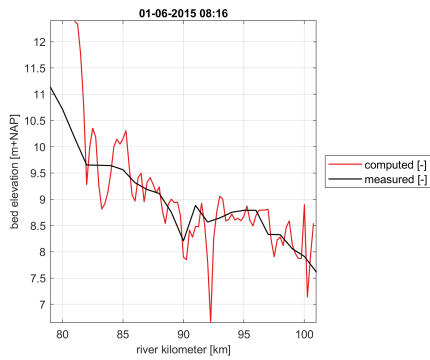
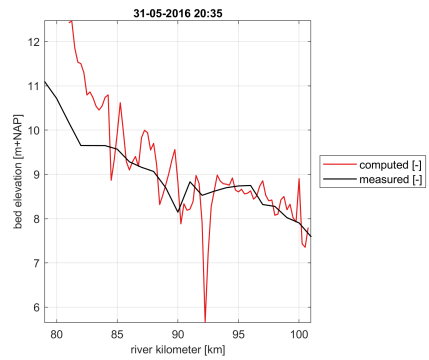


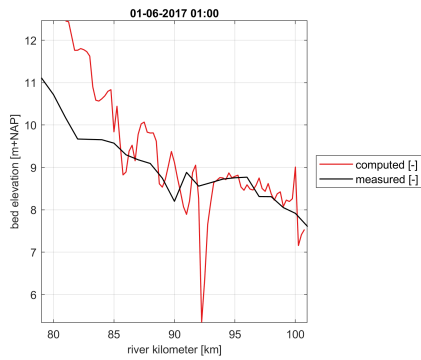
Figure 4.6 Initial bed levels in the model



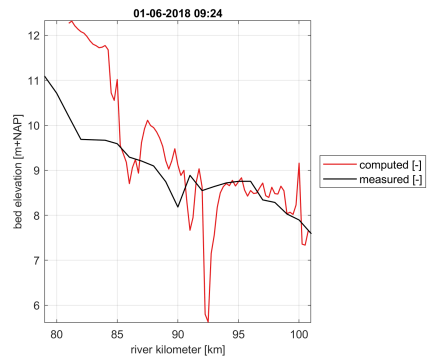
(a) After 1 year



(b) After 2 years

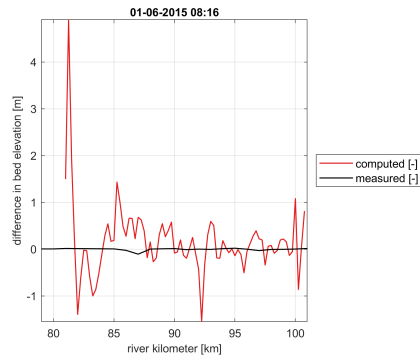


(c) After 3 years

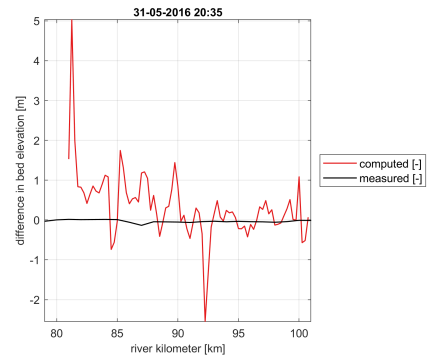


(d) After 4 years

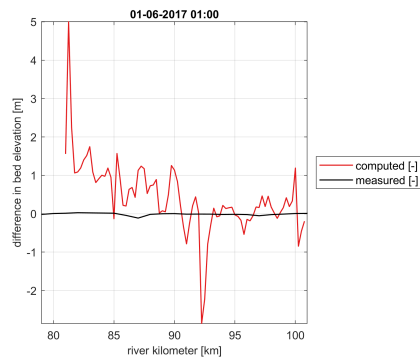
Figure 4.7 Average bed levels per river kilometre



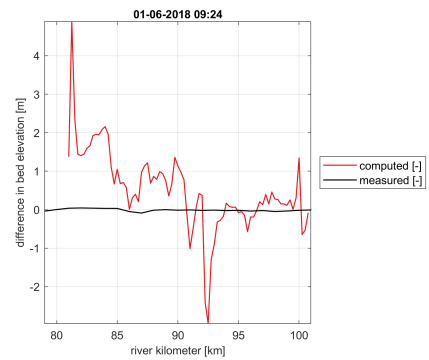
(a) After 1 year



(b) After 2 years



(c) After 3 years



(d) After 4 years

Figure 4.8 Average bed level changes per river kilometre (bed level of indicated year minus initial bed level)

4.2.3 Outlook 2024

The model tests have provided valuable insights into improving morphological simulations. The next step will involve a meticulous analysis and adjustment of the hydraulic, sediment transport, and morphological parameters, alongside further integration of measurements into the analyses.

Reproducing the hydrodynamic conditions and the initial sediment transport is crucial for subsequent replication of morphological developments. Furthermore, expanding the simulation to cover various time periods will be essential for comprehensive calibration and validation.

4.3 Belfeld-Sambeek

4.3.1 Offline sediment transport

Using a model with a fixed bed an estimate for the sediment transport is derived. While running the hydrodynamic model with a fixed bed, stability issues emerged at the downstream boundary. Figure 4.9 shows the incorrect velocity pattern at the downstream boundary. This issue arose because the grid was clipped upstream of the sluice (see Figure 4.10; red arrow is the location of the sluice doors, green arrow points to the location of the boundary; the blue line shows the general flow direction). The fixed weirs at the sluices of Sambeek were hereby lacking in the 20 m simulation, allowing an inflow through the downstream boundary.

While this incorrect pattern did not appear in the 40 m grid model, it did pose issues in the 20 m grid model. Addressing this, the problem was circumvented by adjusting the bed levels at the boundary location. However, adjustments to the model extension and, consequently, the grid and schematization are necessary for this particular reach, and if needed, for the connected reaches. It is worth noting that no stability problems were encountered in the connected reaches during this study.

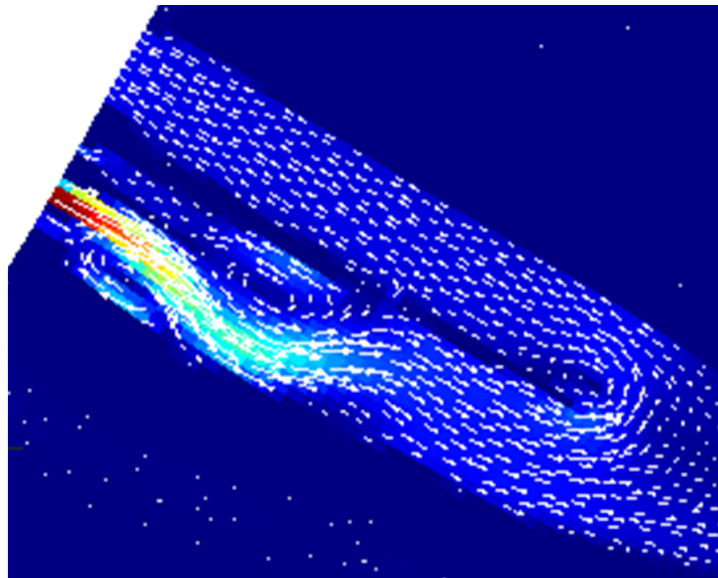


Figure 4.9 Incorrect velocity pattern at the downstream boundary

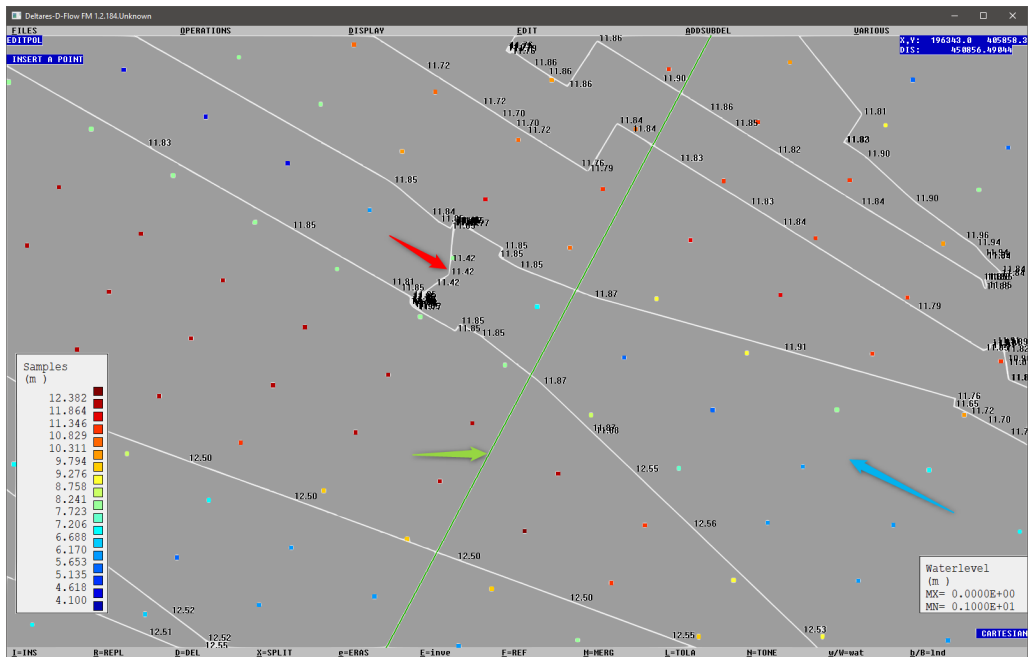


Figure 4.10 Weirs at the downstream boundary

The Meyer-Peter and Müller (1948) formula and settings, including a hiding-exposure correction for the critical shear stress of the different particles. This model is based on the actual river information as known in 2014 (j14). By combining different steady-state discharge simulations and the frequency of occurrence of discharges as found for the period between 2014 and 2018, a total transport per year is calculated. The average data inside the polygon of the main channel is used to compute the sediment transport rate.

Figure 4.11 depicts the calculated annual sediment transport based on the step hydrograph (Figure 3.5).

Significant alterations in sediment transport are observed, potentially suggesting unrealistic outcomes, prompting the need for further investigation.

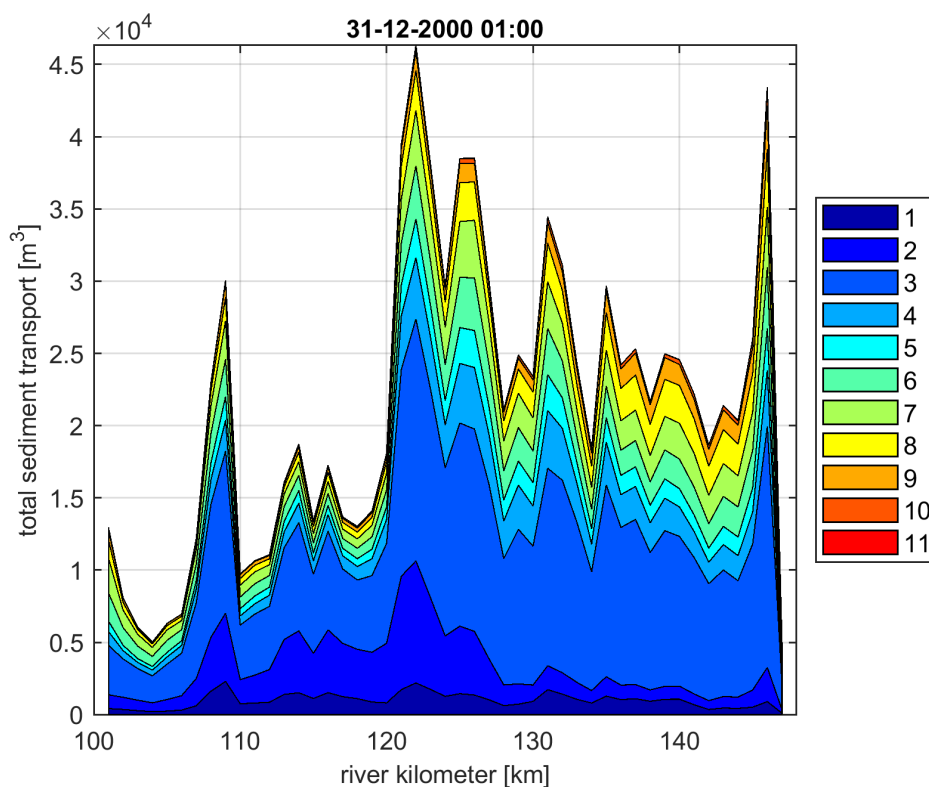


Figure 4.11 Yearly sediment transport considering the standard parameters in the relation by Meyer-Peter and Müller (1948) and ASKLHE=0.65. The colours show the relative contribution of the different sediment fractions.

4.3.2 Morphological test 2014-2018

In alignment with the sediment transport gradients shown in Figure 4.11, the alterations in bed level after the first simulation year (Figure 4.12 to Figure 4.15) indicate potentially unrealistic values for erosion and sedimentation within this reach. Consequently, a comprehensive analysis of the hydraulic, sediment, and morphological parameters needs to be conducted. Nonetheless, the model is running without stability issues.

To assess the realism of the model results, the bed level developments in the model are compared with the measurements. The average initial bed levels measured per river kilometre are compared to those applied in the model. As shown in Figure 4.16, differences exist between these bed levels. Particularly, a significant difference is observed between km 115 to km 120. Therefore, a closer examination is necessary to understand the disparities between the measurements and the initial bed levels in the morphological models.

The computed bed levels using the model after 1 year are depicted in Figure 4.17 alongside the corresponding measured bed levels. Additionally, Figure 4.18 illustrates the bed level changes after 1 year (bed level year minus initial bed level). As evident from these figures, the model computes unrealistic bed level changes. These differences arise from variations in the initial conditions and substantial sediment transport gradients.

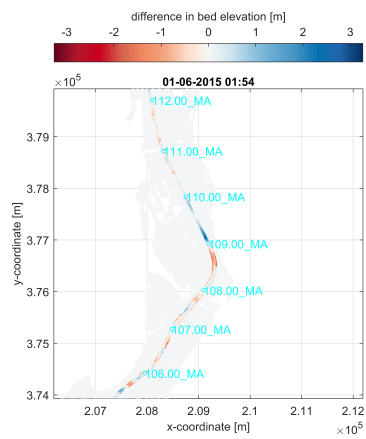
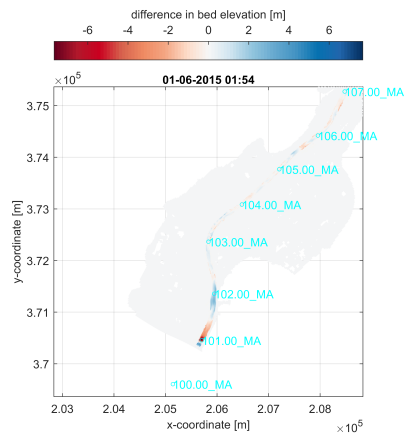


Figure 4.12 Bed level changes km 101 - km 112 after 1 year

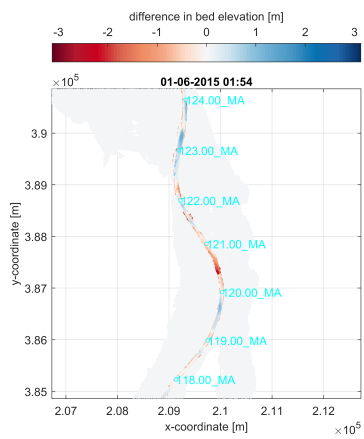
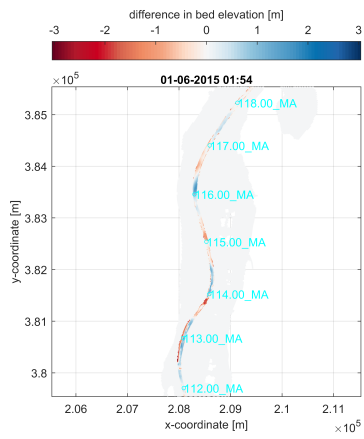


Figure 4.13 Bed level changes km 113 - km 124 after 1 year

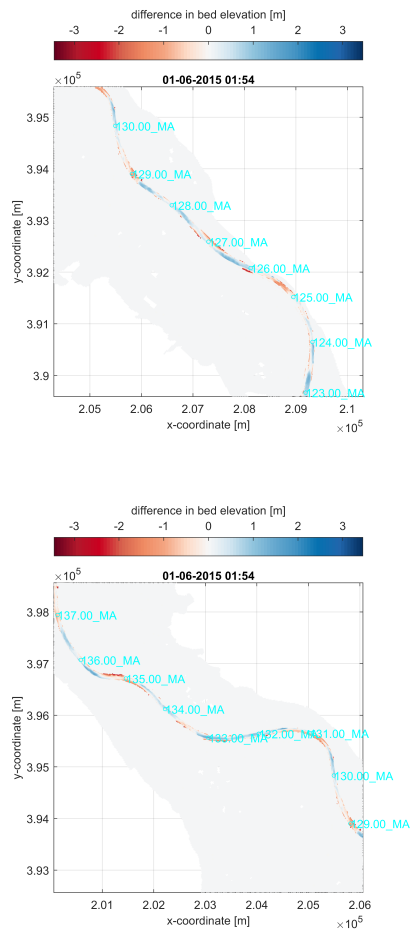


Figure 4.14 Bed level changes km 125 - km 136 after 1 year

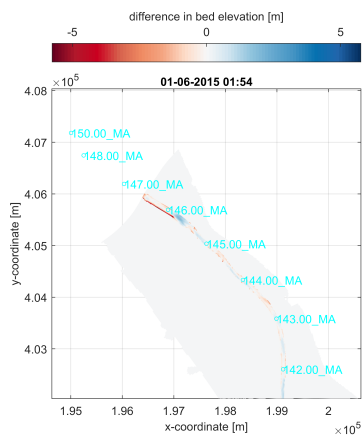
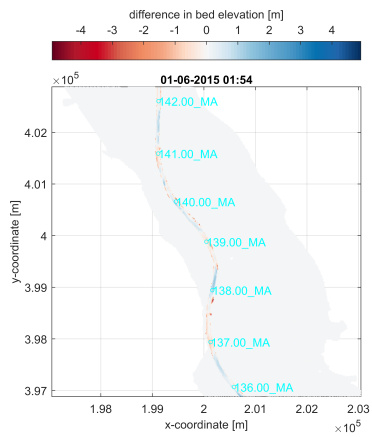


Figure 4.15 Bed level changes km 137 - km 148 after 1 year

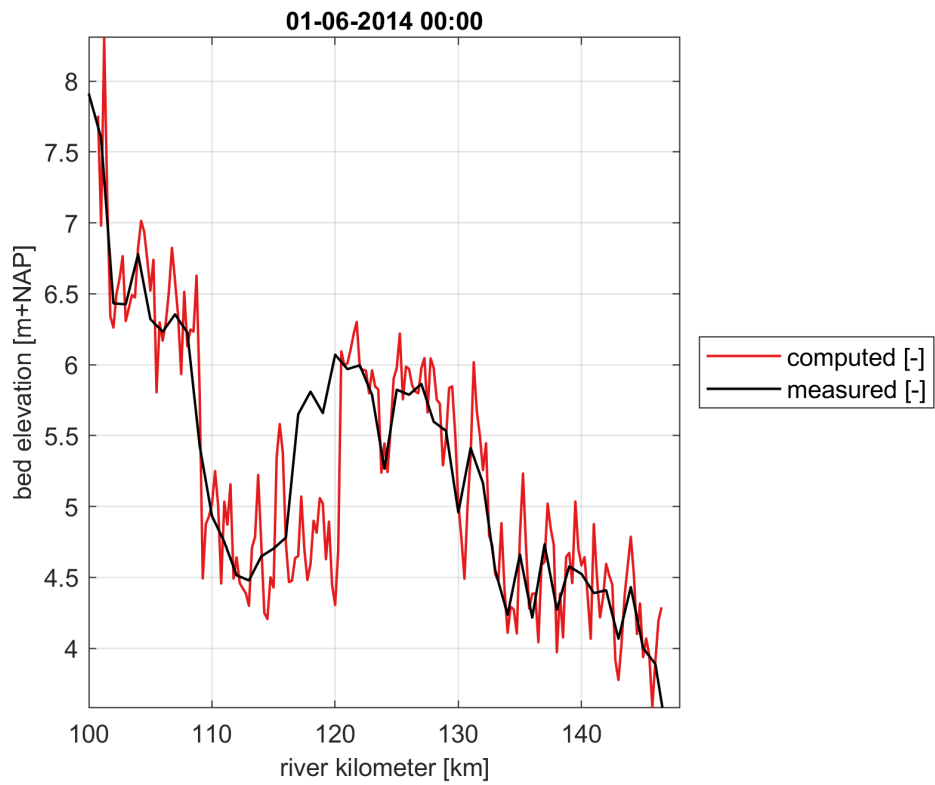


Figure 4.16 Initial bed levels in model and from measurements

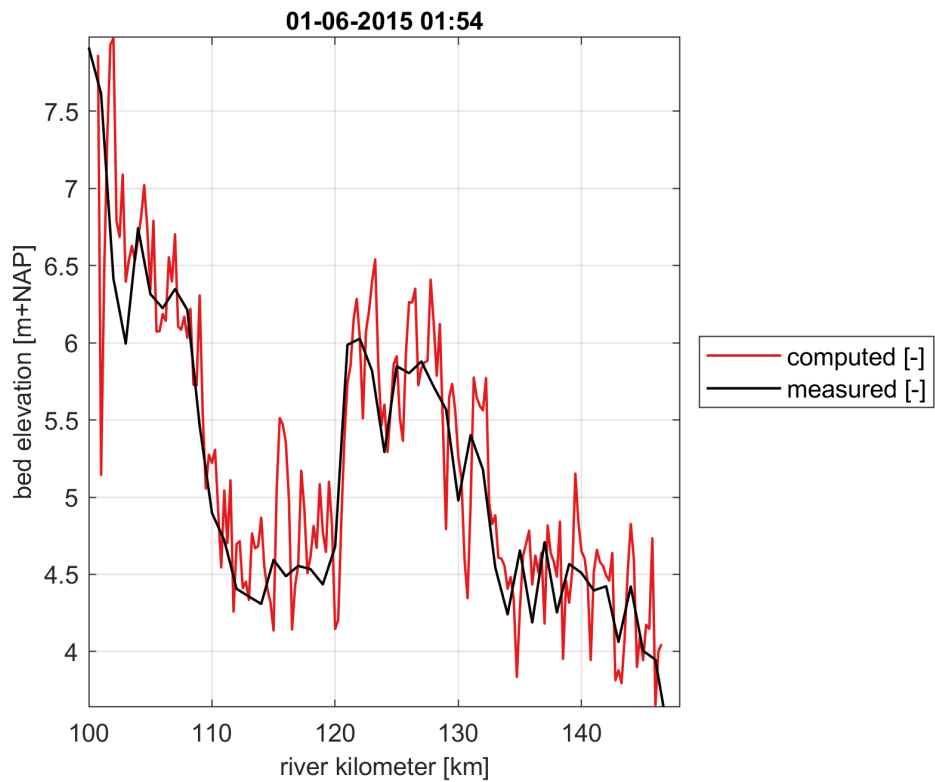


Figure 4.17 Average bed levels per river kilometre after 1 year

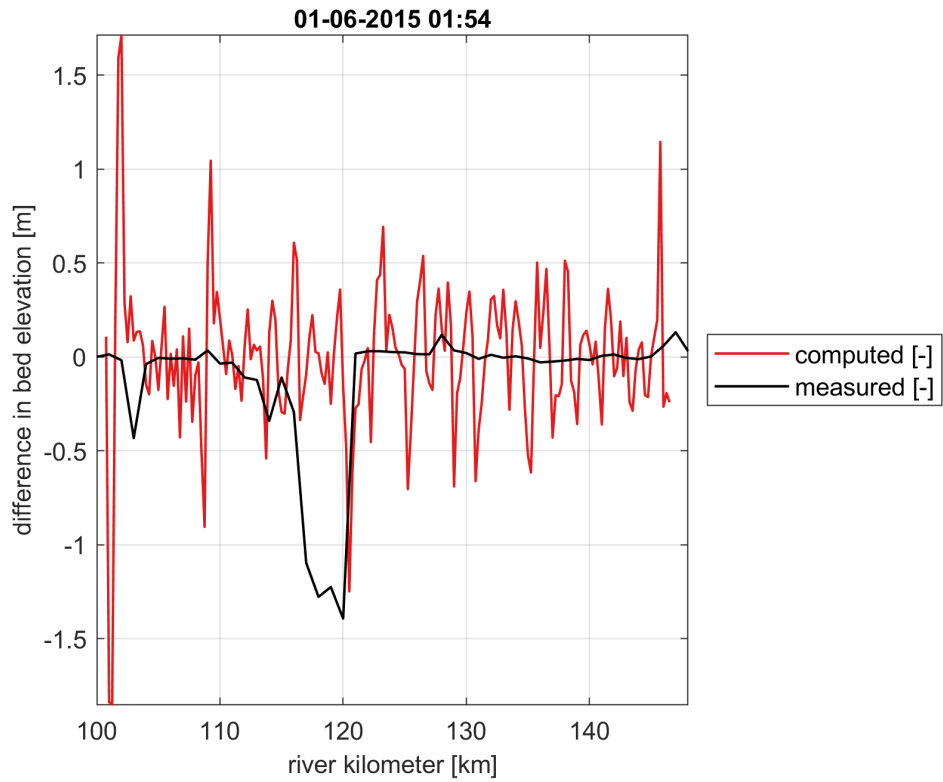


Figure 4.18 Average bed level changes per river kilometre (Bed level year minus initial bed level)

4.3.3 Outlook 2024

The model tests have provided valuable insights into improving the morphological simulations. Initially, extending the model limits downstream is necessary to prevent stability issues caused by the weirs at Sambeek. Once these improvements have been made, the next step will involve identifying additional areas where realistic bed developments are not represented accurately. This will involve incorporating measurements into the analyses. Furthermore, expanding the simulation to encompass different time periods will be essential for comparison and validation.

4.4 Grave-Lith

4.4.1 Offline sediment transport

Using a model with a fixed bed an estimate for the sediment transport is derived. The Meyer-Peter and Müller (1948) formula and settings, including a hiding-exposure correction for the critical shear stress of the different particles are applied. This model is based on the actual river information as known in 2014 (j14). By combining different steady-state discharge simulations and the frequency of occurrence of discharges as found for the period between 2014 and 2018, a total transport per year is calculated. The average data inside the polygon of the main channel is used to compute the sediment transport rate.

Figure 4.19 depicts the calculated annual sediment transport based on the step hydrograph (Figure 3.5).

The variations in sediment transport are generally smooth, except within the initial 5 kilometres of the reach. This discrepancy suggests potential unrealistic outcomes, requiring further investigation.

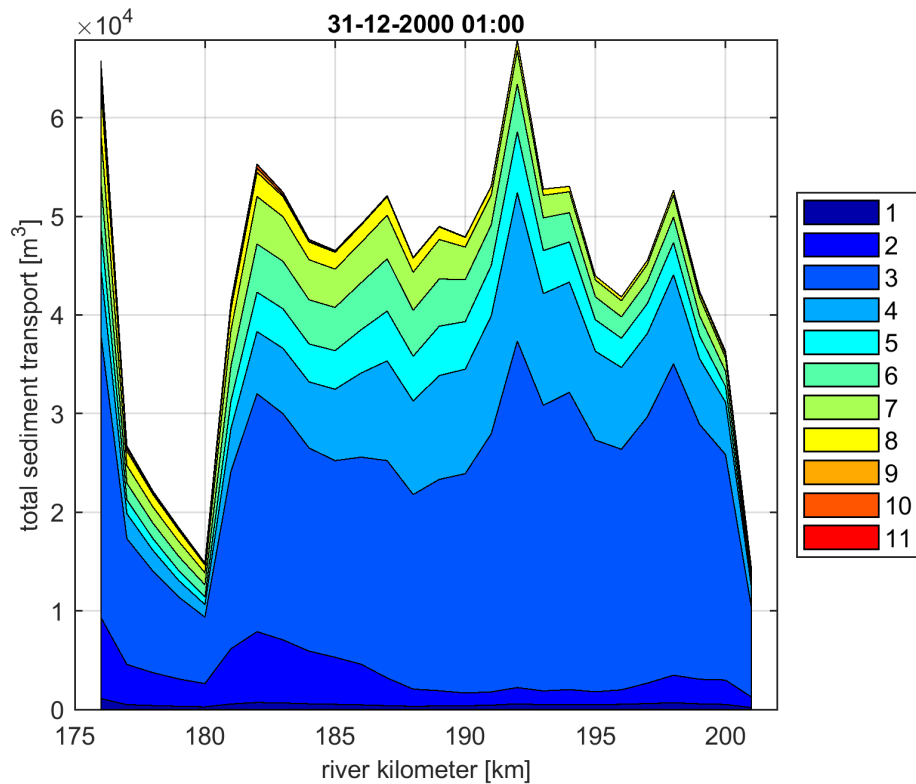


Figure 4.19 Yearly sediment transport considering the standard parameters in the relation by Meyer-Peter and Müller (1948) and ASKLHE=0.65. The colours show the relative contribution of the different sediment fractions.

4.4.2 Morphological test 2014-2018

In alignment with the sediment transport gradients shown in Figure 4.19, the alterations in bed level after the first simulation year (Figure 4.24) indicate potentially unrealistic values for erosion and sedimentation within this reach. Consequently, a comprehensive analysis of the hydraulic, sediment, and morphological parameters needs to be conducted. Nonetheless, the model has operated without stability issues throughout the entire 4-year period. Figure 4.24 shows the bed level changes after 4 simulation years.

In alignment with the sediment transport gradients shown in Figure 4.19, the alterations in bed level after the first simulation year (left plots in Figure 4.20 and Figure 4.21) and after 4 years, (right plots in the same figures) indicate potentially unrealistic values for erosion and sedimentation in the first 5 kilometres within this reach. Consequently, a comprehensive analysis of the hydraulic, sediment, and morphological parameters needs to be conducted. Nonetheless, the model has operated without stability issues throughout the entire 4-year period.

To assess the realism of the model results, the bed level developments in the model are compared with the measurements. The average initial bed levels measured per river kilometre are being compared to those applied in the model. As shown in Figure 4.22, the bed levels in the model are similar to the measured ones.

The computed bed levels using the model for 1, 2, 3, and 4 years are depicted in Figure 4.23 alongside the corresponding measured bed levels. Additionally, Figure 4.24 illustrates the bed level changes after 1, 2, 3, and 4 years (bed level year - initial bed level). As can be observed from these figures, the model computes realistic bed level changes except for the first 5 kilometres. These differences arise from variations in sediment transport gradients.

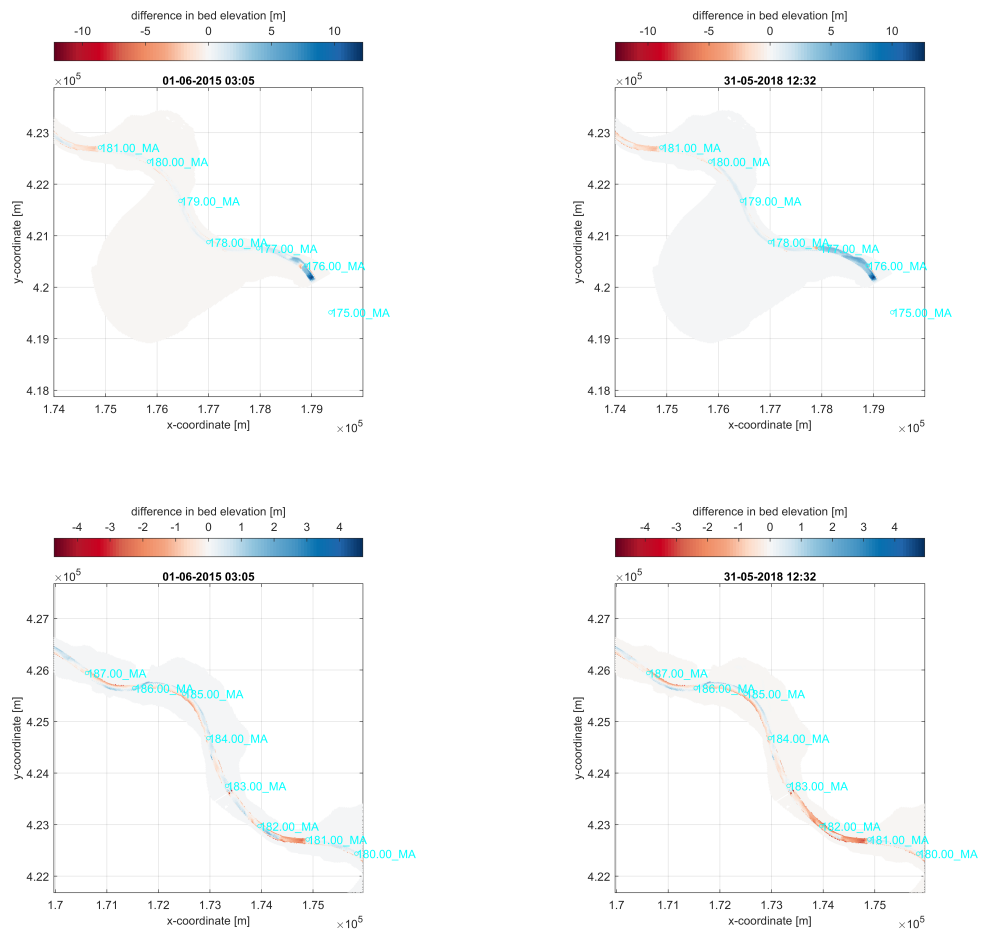


Figure 4.20 Bed level changes km 176 - km 186 after 1 year (left) and after 4 years (right)

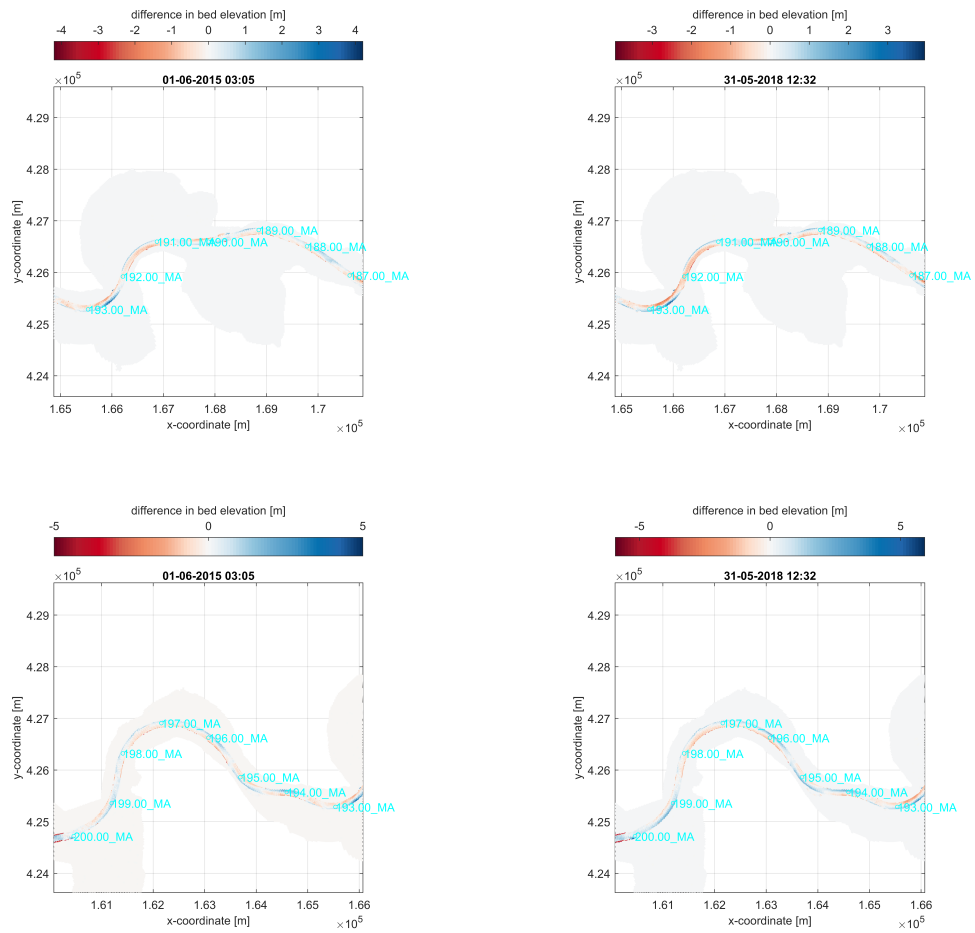


Figure 4.21 Bed level changes km 187 - km 200 after 1 year (left) and after 4 years (right)

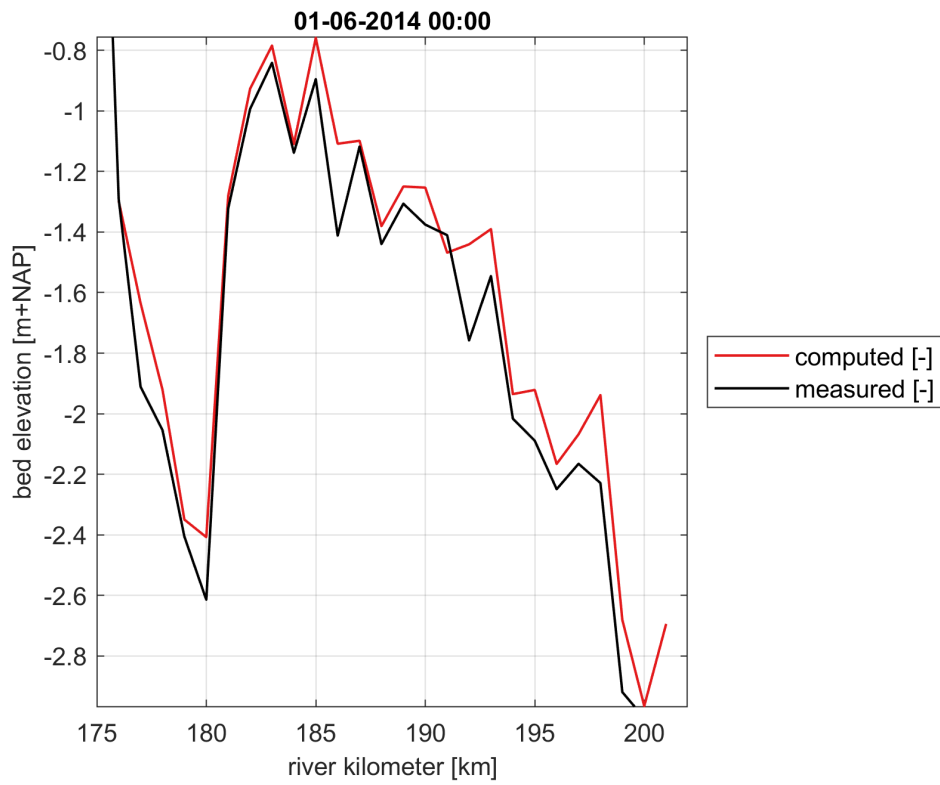
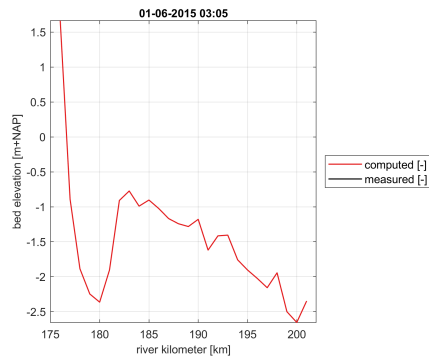
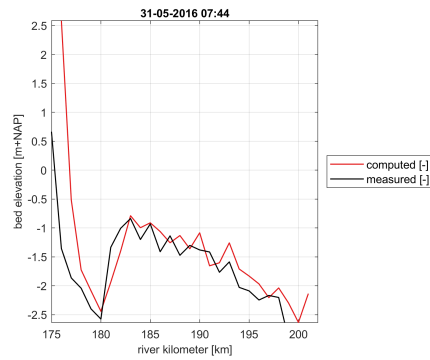


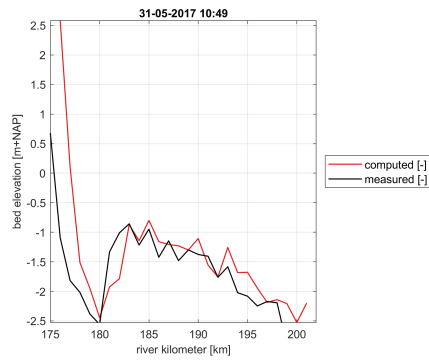
Figure 4.22 Initial Bed levels model and measurements



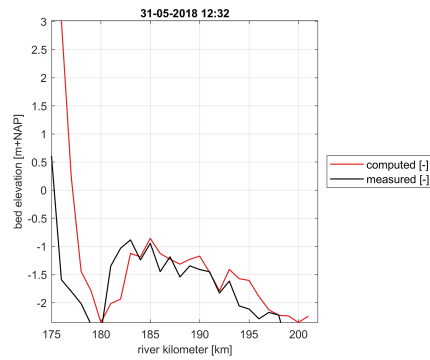
(a) After 1 year



(b) After 2 years

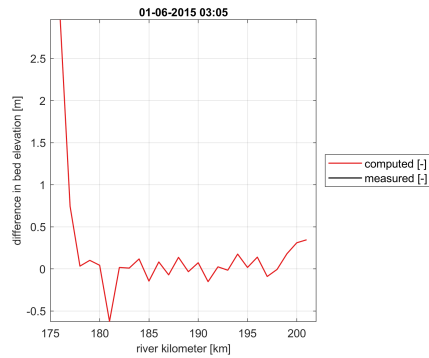


(c) After 3 years

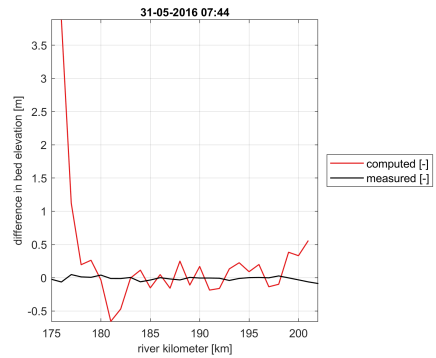


(d) After 4 years

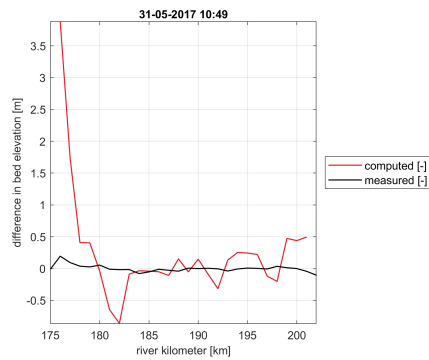
Figure 4.23 Average bed levels per river kilometre



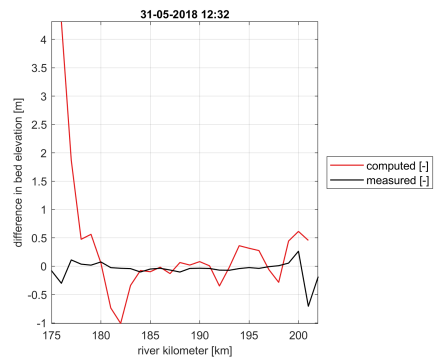
(a) After 1 year



(b) After 2 years



(c) After 3 years



(d) After 4 years

Figure 4.24 Average bed level changes per river kilometre (bed level of indicated year minus initial bed level)

4.4.3 Outlook 2024

Further investigation is needed for the hydrodynamic, sediment, and morphological parameters especially within the initial 5 kilometres of the reach to enhance the accuracy of morphological computations.

4.5 Lith-Keizersveer

4.5.1 Offline sediment transport

Using a model with a fixed bed an estimate for the sediment transport is derived. The Meyer-Peter and Müller (1948) formula and settings were used, including a hiding-exposure correction for the critical shear stress of the different particles. This model is based on the actual river information as known in 2014 (j14). By combining different steady-state discharge simulations and the frequency of occurrence of discharges as found for the period between 2014 and 2018, a total transport per year is calculated. The average data inside the polygon of the main channel is used to compute the sediment transport rate.

Figure 4.25 depicts the calculated annual sediment transport based on the step hydrograph (Figure 3.5).

The sediment transport displays local abrupt changes, specially at km 230. These varying gradients in sediment transport—both positive and negative—will lead to significant alterations in erosion and sedimentation patterns, depending upon the composition of the bed.

An analysis must be conducted to verify the plausibility of these sediment gradient patterns and absolute values. These analyses involve not only analysis of the sediment parameters but also hydrodynamics, as changes in velocities significantly influence sediment transport. Particularly in this downstream part of the River Meuse, the tide might play a role. According to Sieben (2022), a tidal range of approximately 0.5140m will increase sediment transport in the downstream direction. This effect has not yet been considered, as evident from Figure 4.25, where sediment transport decreases in the last kilometres of the reach.

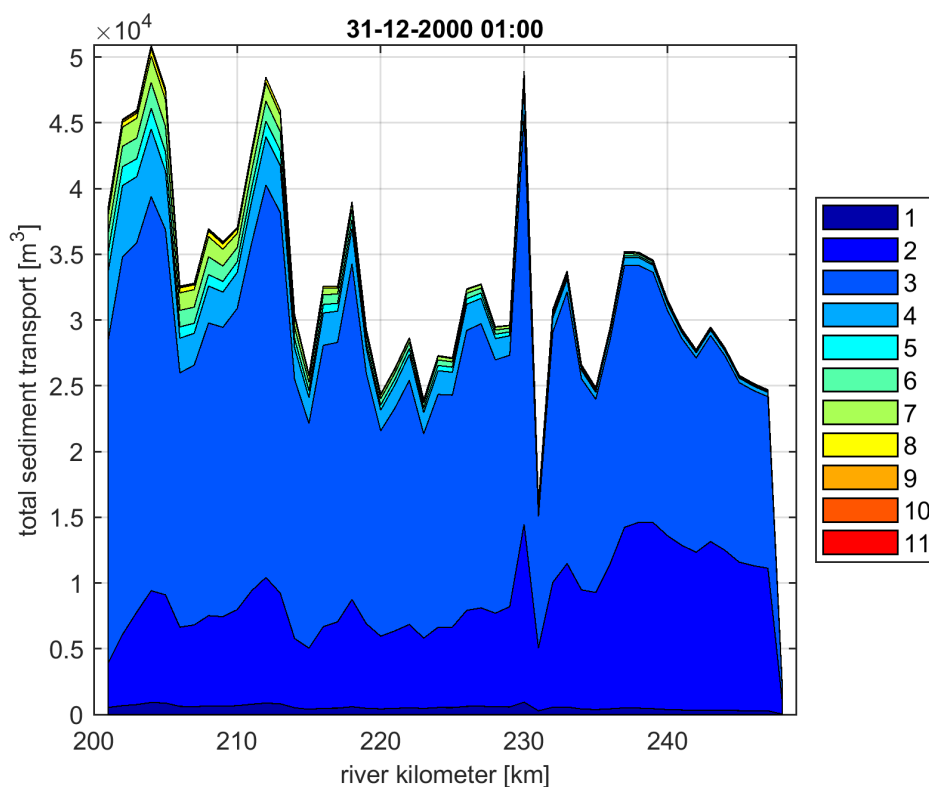


Figure 4.25 Yearly sediment transport considering the standard parameters in the relation by Meyer-Peter and Müller (1948) and ASKLHE=0.65. The colours show the relative contribution of the different sediment fractions.

4.5.2 Morphological test 2014-2018

In alignment with the sediment transport gradients shown in Figure 4.25, the alterations in bed level after the first simulation year (left plots in Figure 4.26 to Figure 4.26) and after 4 years (right plots in the same figure) indicate potentially unrealistic values for erosion and sedimentation within this reach. Consequently, a comprehensive analysis of the hydraulic, sediment, and morphological parameters needs to be conducted. Nonetheless, the model has operated without stability issues throughout the entire 4-year period.

To assess the realism of the model results, the bed level developments in the model are compared with the measurements. The average initial bed levels measured per river kilometre are compared to those applied in the model. As shown in Figure 4.30, there are some differences between these bed levels. Therefore, a closer examination is necessary to understand the disparities between the measurements and the initial bed levels in the morphological models.

The computed bed levels using the model for 1, 2, 3, and 4 years are depicted in Figure 4.31 alongside the corresponding measured bed levels. Additionally, Figure 4.32 illustrates the bed level changes after 1, 2, 3, and 4 years (bed level of the indicated year minus initial bed level). These figures depict a resemblance between the model results and the measured data from km 205 to km 223. However, there are unrealistic sedimentation calculations upstream. Downstream of the reach, the model calculates a significant amount of sedimentation, but this does not align with the measurements. These differences arise from variations in the initial conditions and substantial positive and negative sediment transport gradients. Furthermore, the impact of tides has yet to be incorporated. As per [Sieben \(2022\)](#), sediment transport is anticipated to increase downstream due to the tidal range. Consequently, accounting for tidal effects on sediment transport might decrease or entirely remove the computed sedimentation.

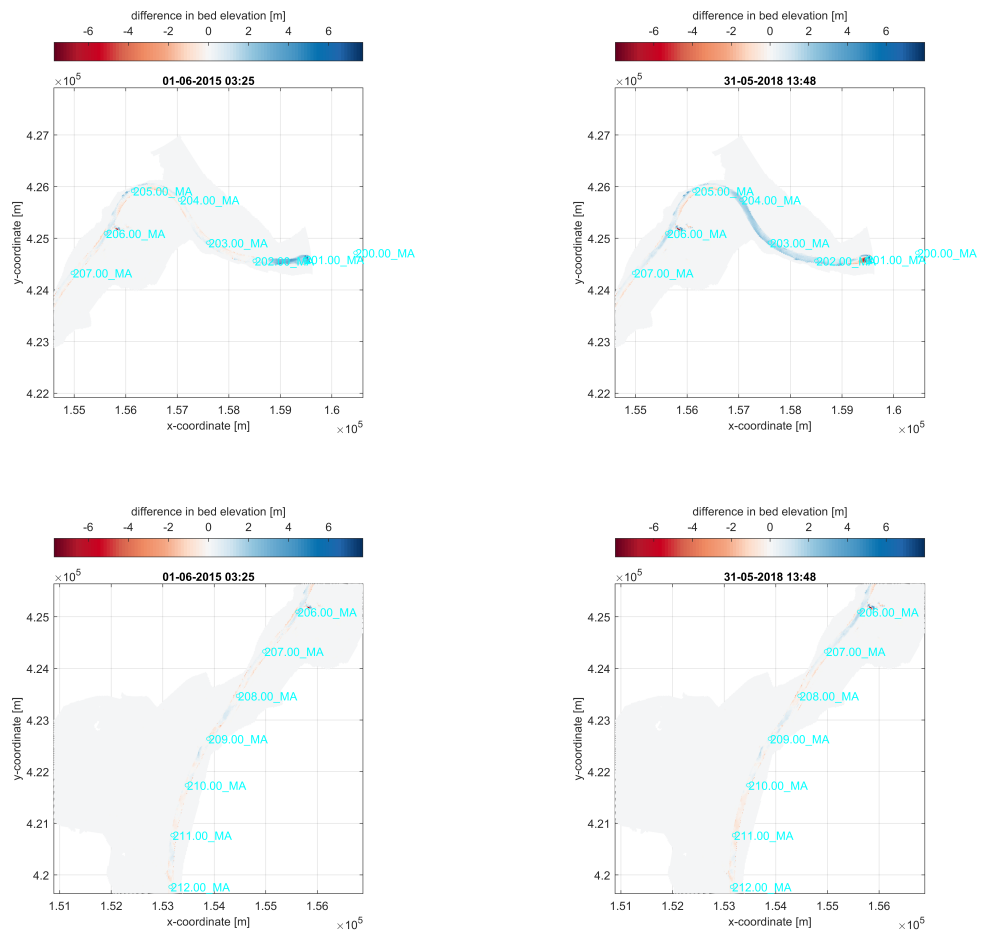


Figure 4.26 Bed level changes km 201 - km 211 after 1 year (left) and after 4 years (right)

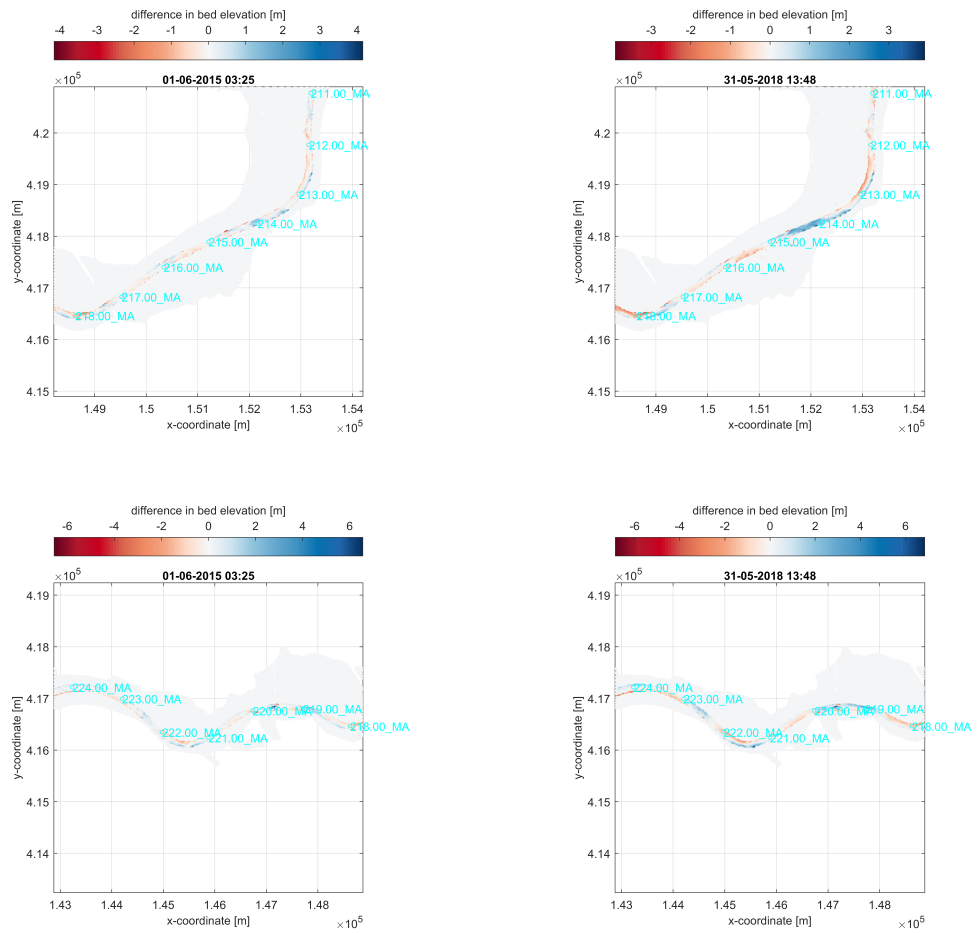


Figure 4.27 Bed level changes km 212 - km 224 after 1 year (left) and after 4 years (right)

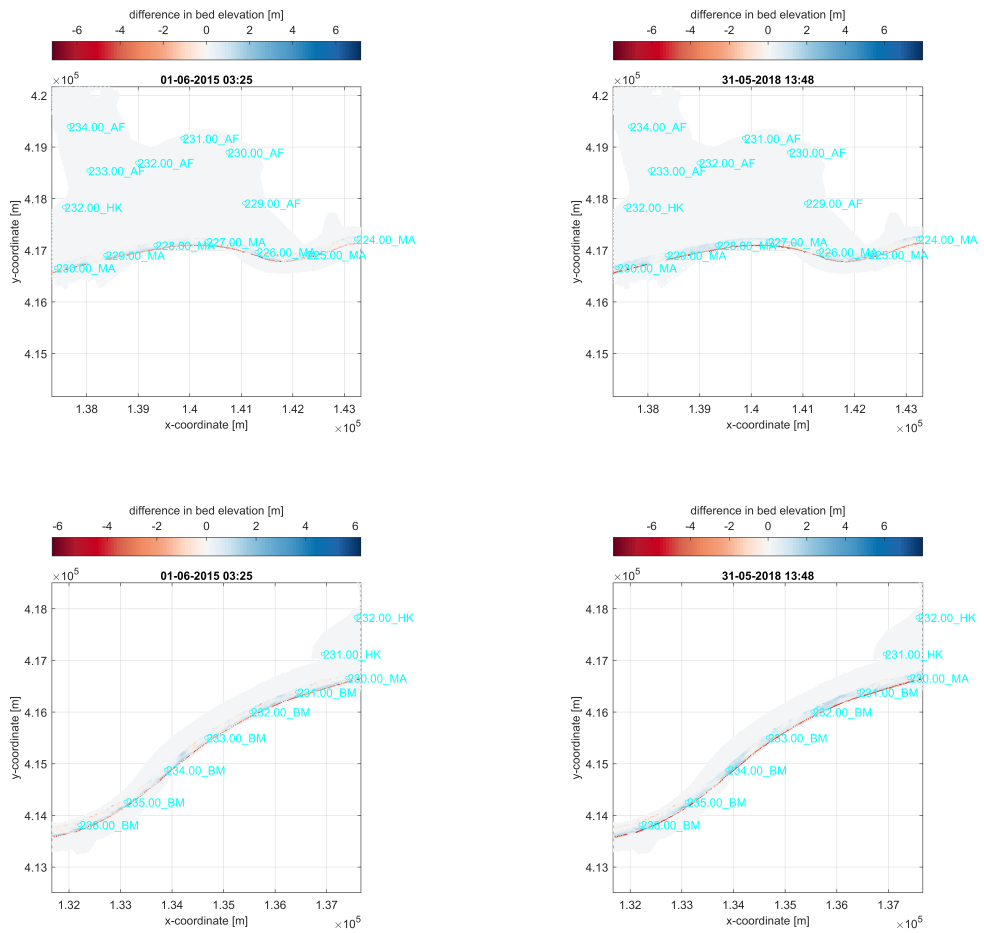


Figure 4.28 Bed level changes km 225 - km 236 after 1 year (left) and after 4 years (right)

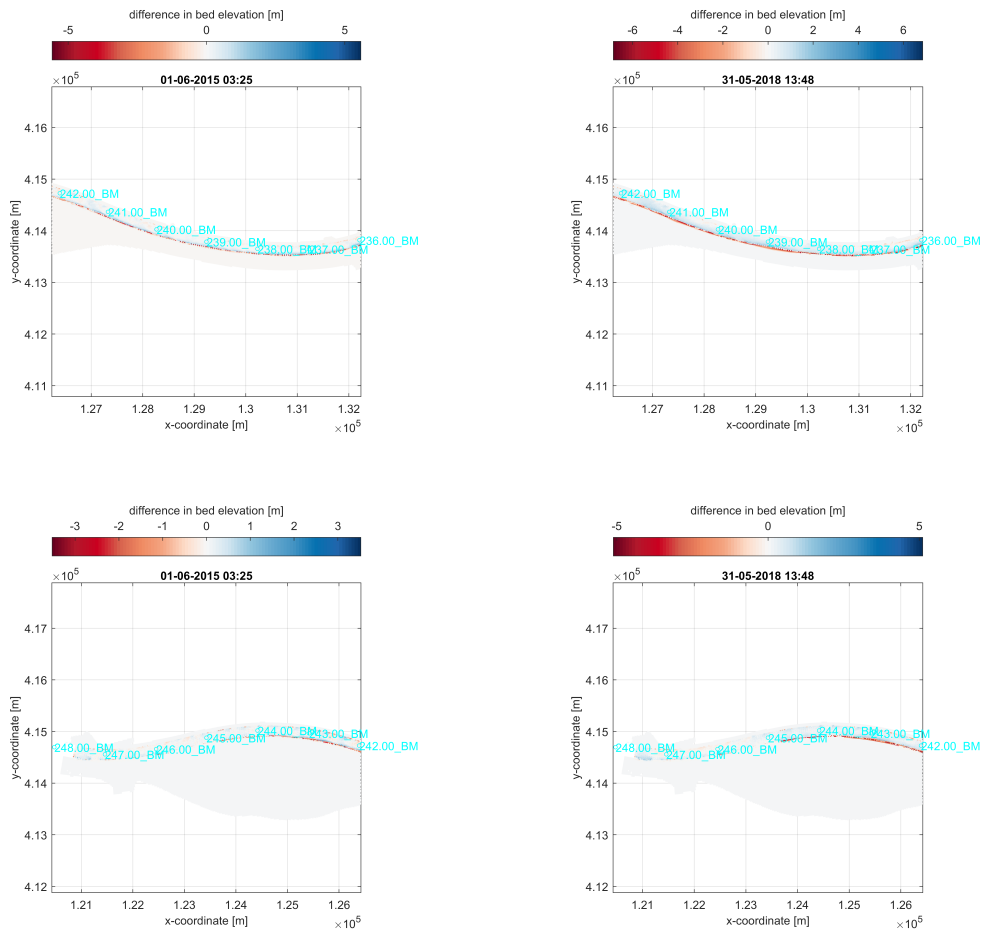


Figure 4.29 Bed level changes km 237 - km 248 after 1 year (left) and after 4 years (right)

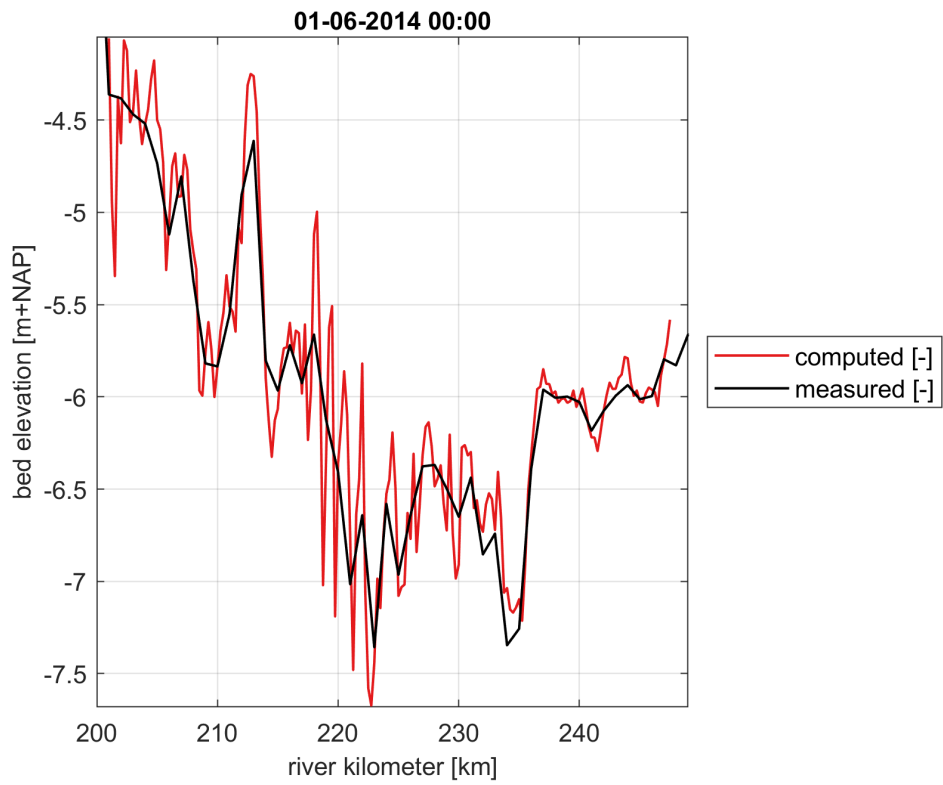
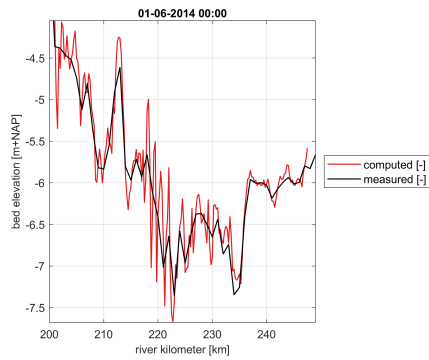
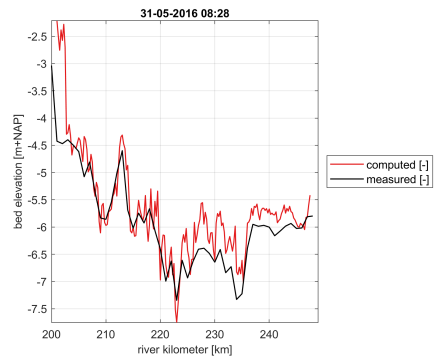


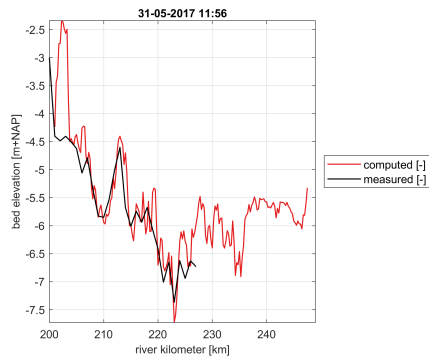
Figure 4.30 Initial bed level in model and from measurements



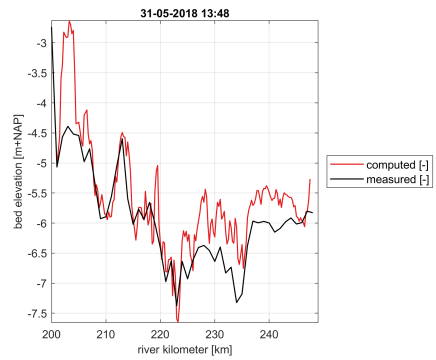
(a) After 1 year



(b) After 2 years

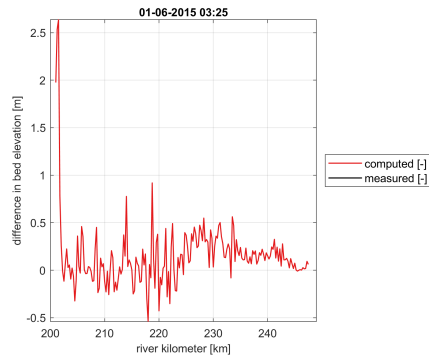


(c) After 3 years

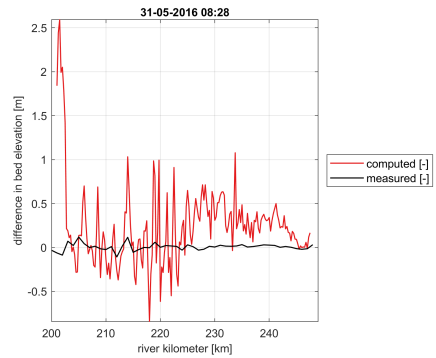


(d) After 4 years

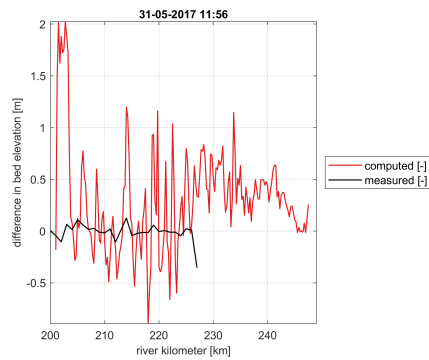
Figure 4.31 Average bed levels per river kilometre



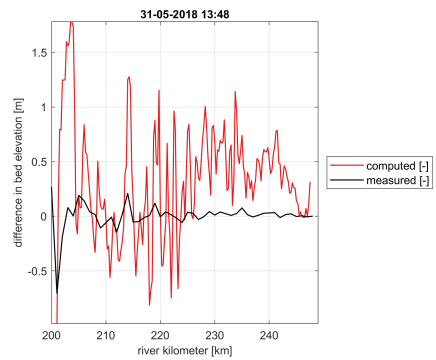
(a) After 1 year



(b) After 2 years



(c) After 3 years



(d) After 4 years

Figure 4.32 Average bed level changes per river kilometre (bed level of indicated year minus initial bed level)

4.5.3 Outlook 2024

The model tests have provided valuable insights into improving morphological simulations. The next step will involve a meticulous analysis and adjustment of the hydraulic, sediment transport, and morphological parameters, alongside further integrating measurements into the analyses. Specifically, further investigation is needed for both the upstream and downstream parts of the model. This entails examining the morphological boundary conditions upstream and considering the influence of tides.

5 Conclusions and recommendations

Morphological models for five reaches of the River Meuse have been constructed: Linne-Roermond, Roermond-Belfeld, Belfeld-Sambeek, Grave-Lith, and Lith-Keizersveer. These models were made by cutting the entire grid with a resolution of 20 m from an existing hydrodynamic schematization. A finer grid resolution becomes necessary to accurately simulate the morphological changes in the main channel. However, due to the computational demands of the finer grid, a coarser resolution, 40 m was utilized to determine the hydrodynamic boundary conditions of the submodels. Presently, there isn't a model of the entire River Maas employing the finer grid resolution. Instead, the river is divided into three submodels to accommodate this higher resolution. As a result, an assumption was made regarding the similarity of the hydrodynamic outcomes between both grids. To test this hypothesis, a visual comparison was conducted between the results obtained from the five hydrodynamic submodels, analyzing water levels and velocities, using both the coarser and finer grid resolutions.

The sediment transport and morphological submodels for these reaches were established using parameters from the Sambeek-Grave model. However, there are differences in the morphological boundary conditions between these reaches and the Sambeek-Grave model. In these five reaches, default boundary conditions have been employed, utilizing equilibrium sediment transport instead of a fixed bed-level boundary as in the Sambeek-Grave model.

The primary objective of this document is to describe the current state of the developed Meuse submodels within the five reaches, identifying the challenges encountered and providing recommendations to improve the prediction of morphological developments. The model status and challenges and recommendations are summarized per submodel in Tables 5.1 and 5.2, respectively.

In general, reproducing the hydrodynamic conditions and the initial sediment transport is crucial for subsequent replication of morphological developments. Furthermore, expanding the simulation to cover various time periods will be essential for comprehensive calibration and validation.

Model	Hydrodynamics	Sediment transport	Morphology
Linne-Roermond	Stable. High velocities at the upstream boundary: Check boundary location. Adjust roughness (smoothness)	Unrealistic gradients	Unrealistic erosion and sedimentation. Run stops after the first simulation year.
Roermond-Belfeld	Stable.	Unrealistic gradients line	Stable. Run 4 years Unrealistic erosion and sedimentation.
Belfeld-Sambeek	Stability issues with the model due to weirs at the downstream boundary. Stability improved following a local bed level correction.	Large sediment transport gradients	Stable. Model is currently running at the time of writing this report. The simulation for the first year reflects similar patterns to the measured data, although more changes are modelled (which could be due to smoothing in the measured data).
Grave-Lith	Stable.	The sediment transport generally appears smooth, except for an abrupt change occurring within the initial five kilometres.	Stable. Run 4 years The simulation results for the four-year period display similarities to the measured data, with the exception of the initial five kilometres of the reach.
Lith-Keizersveer	Stable.	The sediment transport generally appears smooth, except for an abrupt change occurring upstream of the reach and around km 230.	Stable. Run 4 years The simulation results show agreement with the measurements except upstream and downstream.

Table 5.1 Overview of model status and challenges

Model	Hydrodynamics	Sediment	Morphology
Linne-Roermond	Check model extension Adjust roughness (smoothness, and locally if required)	Adjust sediment thickness and bed composition	Change boundary conditions to fixed bed
Roermond-Belfeld	Check model extension Adjust roughness (smoothness, and locally if required)	Adjust sediment thickness and bed composition	Check and if necessary adjust initial bed levels Change boundary conditions to fixed bed
Belfeld-Sambeek	Further check and adjust the model extension downstream Adjust roughness (smoothness, and locally if required)	Adjust sediment thickness and bed composition	Check and if necessary adjust initial bed levels Change boundary conditions to fixed bed
Grave-Lith	Check model extension Adjust roughness (smoothness, and locally if required) if needed the first 5 kilometres	Adjust sediment thickness and bed composition if needed in the first 5 kilometres	Change boundary conditions to fixed bed
Lith-Keizersveer	Check model extension Adjust roughness (smoothness, and locally if required) Investigate the influence of tide and if necessary include it in the model	Adjust sediment thickness and bed composition Investigate the influence of tide and if necessary include it in the model	Change boundary conditions to fixed bed

Table 5.2 Overview of recommendations (outlook)

6 References

- Barneveld, H. J., E. Mosselman, V. Chavarrías and A. J. F. Hoitink, 2024. "Accuracy Assessment of Numerical Morphological Models Based on Reduced Saint-Venant Equations." *Water Resources Research* 60 (1): e2023WR035052. DOI: <https://doi.org/10.1029/2023WR035052>, URL <https://agupubs.onlinelibrary.wiley.com/doi/abs/10.1029/2023WR035052>. E2023WR035052 2023WR035052.
- Berends, K., R. Daggenvoorde and K. Sloff, 2020. *Morphological models for IRM: Meuse 1D*. Tech. Rep. 11203684-015-ZWS-0016, Deltares and HKV.
- Berkhout, W. A., 2003. *Modelling of large-scale morphological processes in sand-gravel rivers. Analytical and numerical analysis of graded morphological processes in the River Meuse*. Master's thesis, Universiteit Twente.
- Chavarrías, V., 2021. *Differences between parallel and sequential simulations*. Tech. rep., Deltares, the Netherlands. Presentation.
- Chavarrías, V. and W. Ottevanger, 2022. *Modelling study of the sediment transport along the Meuse River during the flood wave of 2021*. Memo 11208012-013-ZWS-0001, Deltares, Delft, the Netherlands.
- Frings, R., 2022. *De bodemsamenstelling van de Maas in 1983 en 2020*. Tech. Rep. only data - report to follow, Rijkswaterstaat.
- de Jong, J., 2021. *Ontwikkeling zesde-generatie Maas-model: Modelbouw, kalibratie en validatie*. Tech. Rep. 11200569-003-ZWS-0014, Deltares, Delft, the Netherlands.
- Meyer-Peter, E. and R. Müller, 1948. "Formulas for bed-load transport." In *Proc. 2nd IAHR World Congress, 6–9 June, Stockholm, Sweden*, pages 39–64.
- Ottevanger, W., 2021a. *Morphological model for the River Meuse: Case Study for the reach Sambeek-Grave*. Tech. Rep. 11206793-014-ZWS-0004, Deltares, Delft, the Netherlands.
- Ottevanger, W., 2021b. *Morphological model for the River Meuse: Plan of action for 2021*. Tech. Rep. 11206793-014-ZWS-0001, Deltares, Delft, the Netherlands.
- Ottevanger, W. and V. Chavarrías, 2022a. *Morphological model for the River Meuse: Case Study for the reach Lixhe-Keizersveer*. Tech. Rep. 11208033-002-ZWS-0005, Deltares, Delft, the Netherlands.
- Ottevanger, W. and V. Chavarrías, 2022b. *Morphological model for the River Meuse: Case Study for the reach Sambeek-Grave*. Tech. Rep. 11208033-002-ZWS-0003, Deltares, Delft, the Netherlands.
- Ottevanger, W., V. Chavarrías, M. Busnelli, A. Omer and C. Eijsberg, 2024. *Morphodynamic model of the Meuse River: Model development*. Tech. Rep. 11209261-002-ZWS-0006, Deltares, the Netherlands.
- Ottevanger, W., V. Chavarrías, S. Giri and E. van der Deijl, 2021. *Morphological model for the River Meuse: Model setup, input visualisation, and future steps*. Tech. Rep. 11206792-003-ZWS-0002, Deltares, Delft, the Netherlands.

- Ottevanger, W., E. Verschelling and S. Giri, 2020. *Initiële modelbouw morfologisch model voor de Maas*. Tech Rep. concept 11205234-003-ZWS-0001, Deltares, Delft, the Netherlands.
- Sieben, A., 2022. *Korte karakteristiek waterstanden Heesbeen en Keizersveer*. Note 11-10-2022, Rijkswaterstaat.
- Sieben, A., 2023. *Bepaling standaardset afvoeren DFAST-MI*. Note 31-08-2023, Rijkswaterstaat.
- Sloff, C. J. and H. J. Barneveld, 1996. *Morfologisch model Zandmaas : MAASMOR 1995*. rapport Deltares, WL Delft Hydraulics, Delft.
- Sloff, C. J. and C. Stolker, 2000. *Calibratie SOBEK-Gegradeerd Zandmaas: voorbereiding voor morfologische berekeningen OTB*. Tech. Rep. Q2589, Delft Hydraulics Laboratory, Delft, the Netherlands.
- Spruyt, A. and W. Ottevanger, 2019. *Plan van aanpak morfologisch model Maas*. rapport, Deltares, Delft.
- Yossef, M. F. M., H. R. A. Jagers, S. van Vuren and A. Sieben, 2008. "Innovative techniques in modelling large-scale river morphology." In M. Altınakar, M. A. Kokpinar, İsmail Aydın, Şevket Cokgor and S. Kirgoz, eds., *Proceedings of the 4th International Conference on Fluvial Hydraulics (River Flow), 3-5 September, Cesme, Izmir, Turkey*. Kubaba Congress Department and Travel Services, Ankara, Turkey.

Deltares is an independent institute for applied research in the field of water and subsurface. Throughout the world, we work on smart solutions for people, environment and society.

Deltares

www.deltares.nl